Radiation Measurements 193 (2026) 107625

Contents lists available at ScienceDirect

Radiation Measurements

journal homepage: www.elsevier.com/locate/radmeas

Review

Scintillation dosimetry for FLASH radiotherapy

Esther Ciarrocchi [a,b,c,1], Ivan Veronese [d,e,*,1]

[a] Department of Physics "E. Fermi", University of Pisa, Largo B. Pontecorvo 3, 56127, Pisa, Italy
[b] National Institute of Nuclear Physics, Pisa Section, Pisa, Italy
[c] Center for Instrument sharing of the University of Pisa (CISUP), University of Pisa, Pisa, Italy
[d] Department of Physics "A. Pontremoli", University of Milan, Via Celoria 16, 20133, Milan, Italy
[e] National Institute of Nuclear Physics, Milano Section, Milano, Italy

ARTICLE INFO

Keywords:
FLASH radiotherapy
Ultra-high dose rate
Dosimetry
Scintillators

ABSTRACT

The use of ultra-high dose rate (UHDR) beams for radiotherapy treatments is currently of great interest, as multiple experimental findings show that they may elicit the so-called *FLASH effect,* an increased sparing of normal tissues while maintaining unaltered tumour control. Dosimetry and beam monitoring in FLASH radiotherapy require a paradigm shift in both instrumentation and methodology compared to conventional radiotherapy, given the specific characteristics of UHDR beams. In this scenario, scintillation detectors have emerged as a valid dosimetric tool, and tens of studies have been published in the past few years. In this review paper, we first recall the general properties of scintillators (e.g., scintillator types, available detector geometries, readout systems, and experimental configurations) and discuss the challenges that arise in the context of scintillation dosimetry, with specific reference to FLASH radiotherapy (e.g., linearity and radiation damage). We then provide a comprehensive overview of the current state of research and development in FLASH scintillation dosimetry, focusing on its most critical aspects. The manuscript concludes with a short comparison to other available technologies and a discussion of the key findings to date and future perspectives.

1. Introduction

In recent years, external beam radiotherapy has witnessed a growing interest in an emerging paradigm known as the FLASH effect. This is a radiobiological phenomenon whereby the administration of radiation at ultra-high dose rates (UHDR, >40 Gy/s for electrons, and presumably even higher for protons) results in a differential response between normal and tumour tissues (Favaudon et al., 2014).

Preclinical studies have demonstrated that delivering therapeutic doses within an ultra-short time window, typically under 100–200 ms, can significantly reduce damage to normal tissues while maintaining unaltered tumour control, thus broadening the therapeutic window of radiation therapy. This effect has been observed across a range of organ systems and animal models, but the biological mechanisms underpinning the FLASH effect remain elusive (Gao et al., 2022; Ma et al., 2024; Rosini et al., 2025).

Recent literature indicates that the UHDR beam parameters (e.g., total delivered dose, overall treatment time, gaps between pulses, etc.) may affect the induction and magnitude of the FLASH effect (Liu et al., 2024a). Consequently, a standardized, quantitative characterization of the beam parameters and their biological correlations is imperative for the safe and effective clinical translation of FLASH radiotherapy (FLASH RT), and this path is fraught with challenges (Romano et al., 2022).

Complete and accurate dosimetric descriptions in radiobiological experiments are often scarce, making reproducibility and retrospective analysis difficult. At the same time, substantial advancements in accelerator and beam delivery technologies are needed to produce UHDR beams with precise temporal and spatial control, and much effort has been dedicated to these developments (Butler et al., 2025; Esplen et al., 2020; Farr et al., 2022; Romano et al., 2022).

In this scenario, accurate dosimetry and effective UHDR beam monitoring strategies are crucial, and require a paradigm shift in instrumentation and methodology compared to conventional radiotherapy (CONV RT), given the significant differences in the physical and dosimetric characteristics of their radiation beams. In a single CONV RT treatment fraction, the mean dose rate is generally equal to

This article is part of a special issue entitled: Scintillators Applications published in Radiation Measurements.

* Corresponding author. Department of Physics "A. Pontremoli", University of Milan, Via Celoria 16, 20133, Milan, Italy
E-mail address: ivan.veronese@unimi.it (I. Veronese).

[1] These two authors contributed equally.

https://doi.org/10.1016/j.radmeas.2026.107625
Received 28 October 2025; Received in revised form 22 January 2026; Accepted 27 January 2026
Available online 27 January 2026

approximately 0.1 Gy per second, the dose per pulse (DPP) is of the order of a few tenths of mGy, and the treatments often last a few or several minutes to deliver the prescribed dose fraction. In contrast, FLASH RT delivers ultra-high dose rates exceeding a mean value of at least 40 Gy/s, often reaching instantaneous dose rates (IDR) above 10^6 Gy/s. Ultra high doses per pulse (UHDP), commonly above 1 Gy, are delivered in each radiation pulse (lasting from nanoseconds to microseconds depending on the accelerator). Therefore, therapeutic doses can be delivered in a single or a few pulses over milliseconds, drastically reducing treatment time (Ashraf et al., 2020).

Conventional dosimeters, such as ionization chambers, long considered the gold standard in CONV RT dosimetry, encounter significant limitations when exposed to UHDR beams due to ion recombination and saturation effects (Di Martino et al., 2005), and this has stimulated new chamber designs and construction strategies suitable for FLASH dosimetry (Di Martino et al., 2022; Gómez et al., 2022). In parallel, novel solid-state detectors and dosimeters are being studied and developed to provide information not only on the total dose delivered during the treatment fraction, but also to measure, in real-time, the various parameters related to the beam time-structure, such as the DPP and IDR, that could play an important role in triggering the FLASH effect (Liu et al., 2024a).

Among the main studied solutions, it is worth mentioning those based on silicon and silicon carbide-based detectors (Large et al., 2024; Medina et al., 2024; Milluzzo et al., 2024; Oancea et al., 2025; Romano et al., 2023), as well as, of course, the diamond detector (Marinelli et al., 2022, 2023). Here, scintillation-based detectors are considered as they may also play a significant role in FLASH dosimetry. The broad class of luminescence-based detectors, of which scintillators are a subgroup, offers, in principle, superior performance in terms of spatial and time resolution, as well as in dose-rate linearity, compared to other types of detectors such as charge-based detectors and chemical dosimeters (Fig. 1, Ashraf et al. (2020)).

Furthermore, scintillating materials with high levels of radiological water equivalence are available, ensuring satisfactory energy independence of their dose-response. Lastly, scintillator-based detectors can enable not only point dose measurements but also the evaluation of two-dimensional (2D) and three-dimensional (3D) dose distributions through imaging approaches (Beddar and Beaulieu, 2016). Doing this over relatively large radiation fields, while minimizing the workload of accelerators and thus avoiding repeated measurements via point dosimeter scans, is a much stricter requirement in FLASH RT compared to CONV RT, especially in terms of radioprotection aspects.

Considering all these interesting features, it is therefore not surprising that research into the development and characterization of scintillator-based detectors for use in FLASH RT is very active, with numerous scientific papers published in recent years, exploring different types of scintillating materials, in different geometries, and using UHDR beams of different qualities. Therefore, we think that a comprehensive review of scintillation-based dosimeters in this field is both timely and necessary.

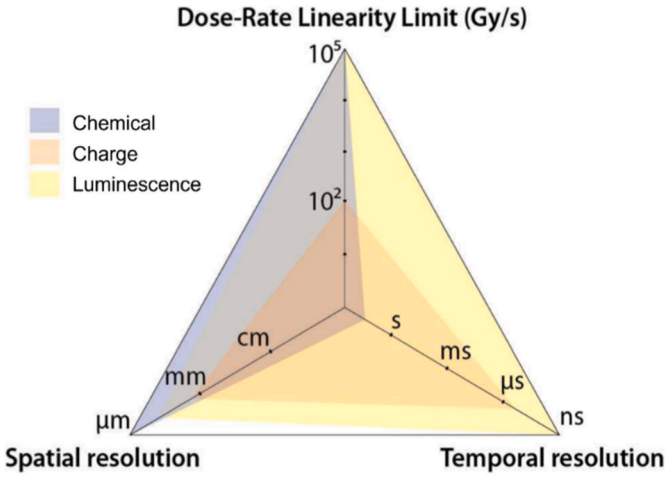

Fig. 1. Spider plot comparing luminescent, chemical, and charge-based dosimeters in terms of dose-rate linearity, spatial and temporal resolution (adapted from Ashraf et al. (2020), licensed under CC BY).

This review aims to summarize the current state of the art in the development, characterization, and optimization of scintillation detectors specifically designed or adapted for UHDR applications. Section 2 is a summary of the general properties of scintillators, including references to the different classes of materials and suitable photodetectors. This section also describes the main geometries that can be adopted for various dosimetric applications, and discusses the challenges that arise in the context of scintillation dosimetry, with specific reference to FLASH RT. The following Section 3 reviews the recent studies on the use of scintillators in FLASH dosimetry and UHDR beam monitoring, focusing on the critical aspects that have been highlighted in Section 2. From this analysis, a discussion of the performance of the scintillators investigated to date, in comparison to that of other systems under study and development for FLASH RT, is finally provided. Through this, we hope to provide a roadmap for researchers working toward the clinical adoption of FLASH RT, offering insights into one of the most promising technologies and identifying key areas where further investigation is needed.

2. General properties of scintillation dosimeters

This section provides a brief overview of the physical properties of scintillating materials and how they can affect their use in dosimeters, especially for UHDR beams. Further insights into the general aspects of scintillators mentioned in this section can be found in various texts, such as Hamel (2021), Lecoq et al. (2017) and Knoll (2010). For more specific details regarding applications in the field of dosimetry, readers are referred to other recent reviews, such as Darafsheh et al. (2024) and Veronese et al. (2024), as well as the book by Beddar and Beaulieu (2016).

2.1. Scintillator types

Scintillator-based detectors can employ organic or inorganic compounds, or even a suitable combination of both. Organic scintillators are typically liquid or plastic, and their scintillation properties are independent of their physical state. They are usually binary or tertiary systems, meaning that the energy absorbed by the matrix is transferred to the organic scintillating molecule, and the de-excitation light of this molecule is detected directly (binary), or after it has been wavelength-shifted to longer wavelengths (tertiary), typically to better match the spectral sensitivity of the photodetector or to minimize the bulk self-absorption. Plastic scintillators are among the most commonly used for dosimetry, and they are obtained by dissolving an organic fluor in a solvent that is then polymerized (Hamel, 2021; Beaulieu and Beddar, 2016).

Inorganic scintillators utilize wide-band-gap materials to convert the energy of ionizing radiation into ultraviolet, visible, or infrared photons. For these materials, scintillation is a relatively complex process, typically divided into three consecutive stages: conversion, transport, and luminescence. During the initial conversion stage, ionizing radiation interacts with the lattice of the scintillator material through a multi-step process. This interaction generates many electron–hole pairs, which become thermalized in the conduction and valence bands, respectively. In the transport stage, these charge carriers migrate through the material. Delays in migration may occur due to the trapping and recapture of charge carriers at defect or impurity levels within the band gap. The final stage, luminescence, involves the radiative recombination of electrons and holes at luminescence centres (Lecoq et al., 2017; Nikl,

2006). Inorganic scintillators are widely studied and employed due to their high density and effective atomic number, as well as high light yield. They are available in various forms, including bulk single crystals, optical ceramics, glasses, thin films, and nanoscale materials, to suit different application scenarios (Anand et al., 2024; Dujardin et al., 2018, 2025; Zhu et al., 2022).

Both classes of scintillators have advantages and disadvantages in the detection of ionizing radiation. Inorganic crystals offer high stopping power, and doping bulk crystals with luminescent impurities can achieve high light yields, albeit with relatively slow scintillation decay times. Moreover, the growth of high-quality inorganic crystals is technically demanding and costly, making large-scale detector fabrication expensive. In contrast, organic scintillators are easier to produce and commercially available in various geometries (as discussed in Section 2.2). They typically exhibit faster response times (decay times on the order of a few nanoseconds) but provide a lower light yield and are more easily damaged by radiation.

The scintillation properties of a material also influence its dosimetric performance. The light yield, for example, determines the detector sensitivity, and, in applications with high fluxes of ionizing radiation, such as external beam dosimetry, the scintillation output is generally sufficient to be easily detected by conventional photodetectors. This is especially true in the case of UHDR irradiations. In contrast, radiation hardness becomes a critical issue during UHDR irradiations, as changes in the luminescence properties of scintillating materials (or of optical fibres in point scintillation detectors) can lead to instability in the dosimeter response, potentially requiring frequent recalibration. The timing characteristics of the scintillation material are generally not critical when the dosimetric quantity of interest is the absorbed dose (for point detectors) or its spatial distribution (for 2D and 3D detectors). This applies in most CONV RT applications, such as small field or reference dosimetry, because the irradiation spans several seconds, which is significantly longer than the decay times of most scintillators, and the time-integrated scintillation signal over the irradiation time is used to retrieve the dose. However, in FLASH RT, the demand for inter-pulse or even intra-pulse dose measurements makes a fast scintillation response an added value.

Recently, there has been growing interest also in hybrid scintillation materials that combine the advantages of both organic and inorganic compounds, including nanocomposite scintillators. These materials are typically composed of plastic matrices doped or coated with scintillating nanocrystals or nanoparticles (Anand et al., 2024), thus combining the high atomic number and radiation hardness of inorganic crystals with the mechanical flexibility and cost-effective fabrication of plastic scintillators. Therefore, they could be particularly useful in applications requiring fast and efficient detection of ionizing radiation (Shevelev et al., 2022), including UHDR dosimetry (Vanreusel et al., 2022).

2.2. Detector geometries and experimental configurations

One of the advantages of scintillators, especially organic ones, is the fact that their geometry, size, and shape can be easily tuned to match the needs of a given application. This can be done on a wide range, from sub-millimetric fibres to large areas and volumes, allowing to span from high-resolution or small field dosimetry to three-dimensional measurements on volumes of tens of cm side. Films as thin as 10 μm can be obtained, at least with plastic scintillators, and small volumes can also be 3D printed (Kapłon et al., 2022), producing various cross-sections. The material where the scintillator is dissolved depends on the final geometry. Plastic scintillating fibres typically feature a polystyrene (PS) core with refractive index n = 1.59, and a thin protective polymethylmethacrylate (PMMA) cladding, with n = 1.42–1.49, smaller than that of the core to guide the light along the fibre via total internal reflection. Larger plastic scintillators are typically based on a polyvinyltoluene (PVT) matrix (n = 1.58). Scintillating fibres are usually coupled to plastic or silica glass optical fibres to serve as light guides to the photodetectors, while larger scintillators are mostly imaged directly.

Historically, fibre-coupled plastic scintillation detectors (PSDs) have probably been the most investigated and developed for dosimetry, with studies comparing the performance of various scintillators, and a few prototypes currently commercially available, such as the Exradin W2 (Standard Imaging, USA), the Hyperscint (Medscint, Canada), or the Blue Physics (BluePhysics, USA) dosimeters. When PSDs are used for remote dosimetry, optical attenuation becomes relevant only over kilometric lengths, while optical coupling losses are always critical for fibre detectors (Ayotte et al., 2006).

A summary of the most common experimental configurations in which scintillation detectors have been tested as FLASH dosimeters is summarized in Fig. 2. Point detectors coupled to optical fibres are usually placed in a thin plastic support used for positioning, centering, and to avoid air gaps (Fig. 2a). They can be irradiated behind layers of water-equivalent plastic or immersed in liquid water. Bidimensional dose mapping can be done in at least three configurations, as shown in Fig. 2b–d. If the 2D transversal dose map is needed, a 45°-degree mirror can be placed after the scintillator to redirect the light to an off-axis camera (Fig. 2b). If the longitudinal dose profile is of interest, e.g., to verify the position of the Bragg peak in a proton beam or to map how the dose decreases with the electron beam penetration, the scintillator screen can be rotated by 90°, so that the longest dimension is on the beam axis, and the scintillation light is imaged laterally (Fig. 2c). Alternatively, the camera can be placed at a certain angle with respect to the beam, to face the first scintillator face that is hit by the beam, and the transversal dose map can be reconstructed after correcting for the geometrical distortions in the image (Fig. 2d). This third 2D configuration seems particularly interesting for clinical use, as the scintillator can potentially be placed on the patient body to verify the entrance dose, provided that the distortions introduced by the curvature of the patient surface are properly compensated for. Finally, the full 3D dose distribution can be recovered with a series of projections, by imaging a scintillator block with multiple cameras (Fig. 2e), and using dedicated reconstruction algorithms to combine them.

2.3. Readout systems

This subsection reports the various readout chains that can be used in conjunction with scintillators. Even though there are no significant differences in the technologies used in FLASH RT vs CONV RT, it is important to point out that, with UHDR beams, time resolution and saturation of the electronics, which are irrelevant at conventional doses and dose rates, may become limiting factors, as will be discussed later in the dedicated Subsection 3.2.

Depending on the intended use, different types of photodetectors can be used to collect the scintillation light. For single-fibre readout, or if time information is relevant, e.g., to monitor the beam pulse time structure, analog detectors such as photomultiplier tubes (PMTs), photodiodes (PDs), avalanche photodiodes (APDs), or silicon photomultipliers (SiPMs) can be chosen.

PMTs and SiPMs have a fast time response and high gain, allowing to detect weak signals. However, they can suffer from a non-linear response with high photon fluxes, making them suboptimal for ultra-high dose rates. PDs may represent the standard solution for high intensity light levels, when no intrinsic signal amplification is necessary. At high rates, also saturation of the readout electronics (e.g., digitizer or electrometer) may need to be taken into account in the detector design.

When imaging is required, digital scientific charge-coupled-device (CCD) or complementary-metal-oxide-semiconductor (CMOS) cameras can be used. Scientific cameras offer the largest dynamic range, can readout multiple fibres and image large areas, but are relatively slow integrating devices, hence are not always able to monitor dynamic signals at the level of the single dose pulse or below. Cameras or CCD linear sensors can also be coupled to spectrographs to measure the spectrum of the collected light via fibre-optic systems.

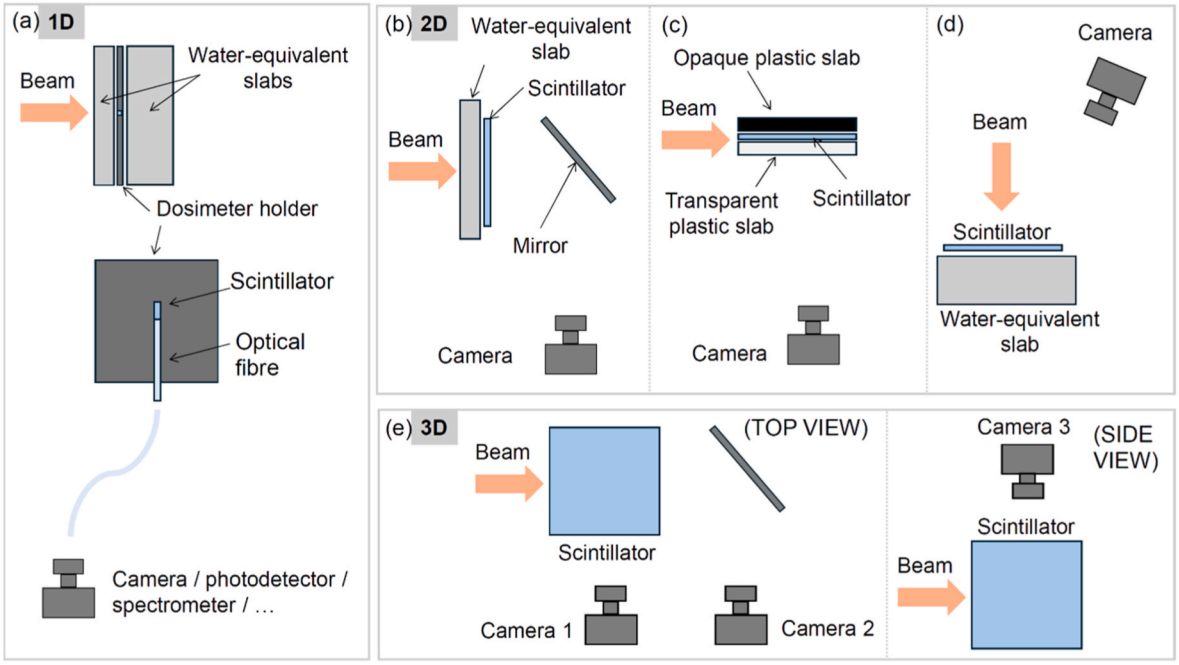

Fig. 2. Configurations for tests of point scintillation detectors (a), 2D detectors (b–d), and 3D detectors (e).

2.4. Challenges and requirements of scintillators for UHDR dosimetry

In order to be suitable for dosimetry, scintillators should provide as many as possible of the following features: stability, reproducibility, linearity with the dose and the dose rate, radiation hardness, high spatial resolution, temperature independence, water equivalence or quantifiable correction factors, apart from being precise and accurate. Correctly evaluating the spurious luminescence (e.g., Cerenkov radiation) is also important, especially when this contribution is a non-negligible fraction of the collected light. Moreover, any quenching of the scintillator emission occurring with particles with high ionization density (i.e., protons or carbon ions) should be properly compensated for, e.g., with Birks' law (Birks, 1951). Of these features, linearity and radiation hardness become of paramount importance for UHDR applications, when high doses and dose rates need to be measured. For beam monitoring, transparency to the beam and real-time feedback are also mandatory. This section provides a brief overview of the key aspects to consider when selecting a scintillation detector for UHDR dosimetry or beam monitoring.

2.4.1. Linearity

The first and foremost desired characteristic of a FLASH dosimeter is a linear response at different dose and dose rate values, which implies that accurate dosimetry can be performed without the need for correction factors. For UHDR electrons, the most common particles used so far in FLASH RT studies, the relevant parameters and typical values are the following (Farr et al., 2022):

- average dose rate (ADR), given by the total dose in the experiment (e.g., 10 Gy) divided by the total irradiation time (e.g., 100 ms)
- dose per pulse (DPP), i.e., the dose in a single beam pulse (e.g., 1 Gy/pulse)
- instantaneous dose rate (IDR), that is the dose per pulse divided by the pulse width (PW), typically a few μs, thus giving IDR $> 10^6$ Gy/s

Ideally, a detector should have a linear response on a broad dynamic range, to be used in both the conventional and UHDR regimes, and it should thus be functioning at DPP values even below 1 mGy/pulse and up to a few Gy/pulse, and be able to sustain IDRs spanning from tens of Gy/s to a few MGy/s. For proton and carbon ion beams, the definition of dose rate is less trivial than for electrons, as a certain point in the treated volume accumulates dose consecutively from the beams of different energies that compose the spread-out Bragg peak, unless specific modulators are used. Moreover, in pencil beam scanning (PBS) irradiations, the cumulative dose at that point is due to different adjacent pencil beams, consecutively passing near it. Hence, several definitions of dose rate have been formulated and are still being investigated (Diffenderfer et al., 2022; Farr et al., 2022; Folkerts et al., 2020).

2.4.2. Time and spatial performance

An innovative requirement in dosimetry for FLASH RT, unnecessary in CONV RT, is the ability of a dosimeter to resolve the temporal structure of the beam, as it may contribute to triggering the FLASH effect. This includes distinguishing the dose delivered by individual radiation pulses, or even monitoring the dose rate within a single pulse (i.e., the IDR). To achieve this, a fast scintillator is required, with decay times much shorter than the interval between consecutive pulses, or even shorter than the pulse duration itself.

Most radiotherapy sources currently under development for FLASH RT are pulsed, with variable repetition rates. In most linear electron FLASH accelerators, beam pulses last on the order of 1–10 μs (typically 3–5 μs) and are delivered every few milliseconds, i.e., with a pulse repetition frequency (PRF) in the range of 100–1000 Hz, typically 200–400 Hz. For cyclotron-based protons, the beam can be considered quasi-continuous, consisting of nanosecond pulses spaced by tens of nanoseconds, corresponding to PRFs on the order of tens to hundreds of MHz (Ashraf et al., 2020; Romano et al., 2022). Protons and carbon ions generated in synchrotron facilities are also delivered in pulses. However, their slow spill extraction, typically lasting up to 100–200 ms (Weber et al., 2022), makes it difficult to reach the ultra-high dose rates required for FLASH RT. As a result, only a limited number of studies have been conducted so far (Tashiro et al., 2022; Tinganelli et al., 2022a, 2022b), and none of them have employed scintillation dosimeters. Finally, laser-driven beams are characterized by a distinct temporal structure, with sub-nanosecond pulses achieved either in single-shot irradiations or at PRFs of 1–10 Hz (Romano et al., 2022).

In CONV RT, the most used radiation are X-rays with energies of a few MeV and produced via bremsstrahlung using linear electron

accelerators. Achieving UHDR photon beams is highly challenging due to the intrinsically low efficiency of the bremsstrahlung process and the need for high electron currents (Farr et al., 2022; Vozenin et al., 2024). Two other approaches currently being tested in preclinical FLASH RT studies involve using (i) X-rays with energies on the order of a few tens of keV, generated by suitably modified X-ray tubes, and (ii) photons produced as synchrotron radiation (Tao et al., 2025). The temporal characteristics of these photon beams are highly variable, and they depend on the specific features of the machine or facility that generated them. In the literature, there are a few examples of studies characterizing scintillation dosimeters conducted with various types of UHDR photon beams (Archer et al., 2019; Hart et al., 2022; Shaharuddin et al., 2021; Vidalot et al., 2022).

Considering this broad spectrum of UHDR beam types under development, the minimum temporal resolution required of a scintillation detector depends on both the type of radiotherapy source and the purpose of the measurement. Furthermore, in the current stage where research in FLASH RT is still dominated by radiobiological and preclinical studies, the dynamics of the biological and chemical processes underlying the FLASH effect (Ma et al., 2024) contribute to defining the needed time performance.

On the basis of these considerations, it cannot be assumed that a single scintillator, or a single technology, will be suitable for all research, dosimetry, and UHDR beam monitoring applications in FLASH RT. Nowadays, organic scintillators offer the best time performance due to their scintillation decay times on the order of nanoseconds. Nevertheless, recent advances in the development of ultrafast inorganic scintillators (Wibowo et al., 2023) and the ongoing search for and characterization of novel hybrid materials (Shevelev et al., 2022) make these alternatives particularly promising as well.

Complementary to the time information is the capability to measure the dose distribution over extended areas or volumes. This is particularly important, for example, in quality assurance or beam monitoring, to confirm that, even at UHDR, the intended dose profile is maintained, and its homogeneity is as expected, or to monitor the dose during *in vivo* experiments (Darafsheh et al., 2024), as this can help correlate the radiobiological effects with the dosimetric beam parameters. The needed spatial resolution is the same as for CONV RT, i.e., it is typically sub-millimetric (Darafsheh et al., 2024) and varies also with the beam size. The diameter of UHDR electron beams is determined by the size of the so-called applicator, a PMMA hollow cylinder that scatters and passively collimates the electrons to provide a flat and symmetrical dose profile in a certain area. As an example, applicator diameters for the ElectronFLASH (SIT, Sordina IORT Technology) range from 10 mm to 120 mm (Di Martino et al., 2023)[2], while proton beams typically have Gaussian profiles with widths of a few millimeters (Kanouta et al., 2024).

2.4.3. Radiation damage

Many variables may affect how a scintillator can be damaged by a certain dose of ionizing radiation, such as the radiation type, the dose rate, and possibly also the presence of oxygen (Kharzheev, 2019), and it is well known that organic ones tend to be more affected. An accurate evaluation of this in FLASH RT dosimetry is necessary and of primary importance for two main reasons. On the one hand, with the new machine technology capable of delivering UHDR beams, doses known to induce sensitivity changes in scintillation dosimeters can now be delivered within seconds, instead of hours or days as in conventional dose rates (Tho et al., 2025), thus significantly shortening the lifetime of detectors. On the other hand, since radiation damage depends on beam characteristics, such as dose rate (see Subsection 3.3), the well-established information on the radiation hardness of scintillation dosimeters obtained in past years with conventional radiotherapy beams, along with the corresponding mitigation strategies, may no longer apply to UHDR beams typical of FLASH RT.

One of the most demanding fields in terms of detector radiation hardness is High Energy Physics (HEP). Therefore, much of the information currently available for various types of scintillators has been derived from studies within this domain.

For organic scintillators, the changes in measured light output following exposure to high doses of ionizing radiation are due to two concurrent phenomena: i) decreased light yield caused by damage to the fluorescent component, and ii) reduced light transmission caused by the creation of optical absorption centres by free radicals. The latter typically manifests as yellowing of the polymer matrix and tends to affect more severely blue-emitting scintillators, which are the most common. This effect is compounded by the long-term degradation of the polymer upon oxygen exposure. Some recovery or annealing of the damage is also observed over periods of hours or days following exposure (Knoll, 2010). In typical plastic scintillators, significant degradation in light yield is seen for cumulative gamma-ray exposures in the range of 10^3–10^4 Gy, whereas more radiation-resistant formulations, including liquid scintillators, show little decrease in light output at gamma doses as high as 10^5 Gy (Beddar and Beaulieu, 2016; Knoll, 2010).

Regarding inorganic scintillators, it is now well established that the most significant damage in the majority of them results from the formation of colour centres within the bulk material, which absorb part of the scintillation light along its path to the photodetector. Since most colour centres absorb in the ultra-violet (UV), crystals that emit at longer wavelengths tend to be less affected. Colour centres are created by the trapping of electric charges at structural defects or impurities in the crystal, and are therefore directly correlated with the quality of the raw material (Lecoq et al., 2017). The luminescence yield may also be modified if luminescence centres undergo transformations under irradiation. The scintillation mechanism itself is very stable in many crystals, particularly in self-activated ones, for which radiation damage is only related to optical transmission loss caused by the formation of colour centres. In contrast, in activated scintillators, both scintillation efficiency and transparency can potentially degrade under irradiation (Lecoq et al., 2017).

Because of the many variables involved in the processes of radiation damage, it is difficult to quantify the exact radiation dose at which measurable damage occurs under specific conditions, but it is well established that some inorganic scintillators (e.g., GSO) are intrinsically more radiation-resistant than others (e.g., thallium-activated alkali halides) (Knoll, 2010). Interestingly, perovskites have demonstrated notable radiation hardness, and perovskite nanocomposite scintillators have shown substantial stability of light yield after gamma-ray exposures up to at least 10^6 Gy (Anand et al., 2024).

Finally, for scintillation dosimeters that use optical fibres to transport the scintillation signal, radiation exposure of the light guide itself can lead to variations in dosimetric response due to fibre damage, particularly in plastic ones. Ionizing radiation alters the structure of the polymers, and free radicals can absorb and scatter scintillation light, reducing the amount of light reaching the photodetector. In addition, colour centres created in the optical fibre absorb light at specific wavelengths, further reducing transmission efficiency (Kharzheev, 2019) and ionizing radiation can also modify the refractive index of the optical fibre, thereby altering its optical properties (Li et al., 2024).

2.4.4. Spurious luminescence

Most scintillation emissions are accompanied by some degree of spurious luminescence, a broad term that covers various forms of visible light generated by materials interacting with ionizing radiation. Among these phenomena are Cerenkov radiation and the intrinsic radioluminescence from irradiated transparent components, such as the optical fibres used in PSDs. For PSDs, the expression *stem effect* is often used, by analogy with the stem of a flower, to describe the parasitic

[2] although so far the FLASH effect *in vivo* has been verified only with electron beam size larger than 2 cm (Farr et al., 2022).

Cerenkov and fluorescence signals produced within the optical fibre and propagated together with the scintillation light.

Cerenkov radiation, bluish-white light emitted when charged particles traverse a dielectric medium at a speed exceeding the phase velocity of light in that medium (Jelley, 1961; Ciarrocchi and Belcari, 2017), is the dominant contribution, and its geometry- and depth-dependence requires dedicated correction methods to correctly retrieve the dose. Several approaches have been developed in the past twenty years, mostly for fibre detectors (Darafsheh et al., 2024; Veronese et al., 2024; Beddar and Beaulieu, 2016). These correction approaches are summarized in Fig. 3, and include: the twin-fibre method (Beddar et al., 1992a, 1992b, 1992c), optical filtering (de Boer et al., 1993), spectroscopic separation, chromatic removal (Fontbonne et al., 2002), and hyperspectral analysis (Archambault et al., 2012; Therriault-Proulx et al., 2012). Time filtering (Clift et al., 2002) and air-core fibres (Lambert et al., 2008) are also possible solutions, but they have not been adopted yet in FLASH dosimetry.

As for Cerenkov removal methods, there have been no significant methodological innovations in the FLASH field with respect to conventional dosimetry, and Cerenkov contamination is presumably not fundamentally altered in the FLASH regime. However, it may become more critical in UHDR settings due to potential changes in the optical properties of the scintillator (e.g., transparency loss) induced by high doses or high dose rates, especially in plastic scintillators with short-wavelength emission. Moreover, not all of the methods traditionally developed for point detectors are readily applicable to other geometries (i.e., 2D and 3D scintillators), and may require specific approaches.

3. State of the art of FLASH scintillation dosimetry

This section reviews the state of the art of the research on scintillation detectors for applications in FLASH/UHDR dosimetry and beam monitoring. A bibliography search was conducted during the last week of August 2025 in the "All Databases" and "All Collections" sections of the Web of Science platform. The search used appropriate Boolean combinations of the terms *scintillator*, *flash*, *dosimeter*, and *radiotherapy* (including their variants, synonyms, and acronyms such as PSD, UHDR, and UHDP) as keywords in the "Topic" field. This query returned a total of 69 records published between 2020 and 2025. The search did not yield any records of works published before 2020. A screening of the results led to the exclusion of 18 records. Of the remaining 51 records, 37 are classified as "article," 3 as "proceeding paper," and 3 as "review article." The rest are categorized as "dissertation thesis," "meeting abstract," or "patent." Among the three published reviews, one is focused on fibre-optic scintillation dosimeters in various radiotherapy applications (Veronese et al., 2024), while the other two are more specific for FLASH RT. Tao et al. (2025) offers a summary of the main devices used to generate UHDR X-rays and describes the detectors reported for their monitoring, while Ashraf et al. (2020) addresses the potential role of luminescent detectors, particularly Cerenkov and scintillation-based detectors, in the development and clinical implementation of FLASH RT. In addition, other reviews discuss the use of different dosimeters, including scintillators, for UHDR dosimetry and for dosimetry of other non-standard radiotherapy sources (Butler et al., 2025; Romano et al., 2022).

The structure of this section follows that of Subsection 2.4, reporting how the different aspects and issues of scintillators have been evaluated. When needed or applicable, results obtained with point detectors and 2D geometries, i.e., scintillating screens, are discussed separately, while 3D detectors, i.e., scintillating blocks, are mentioned only for measuring the spatial dose distribution (Subsection 3.2). A final subsection (Subsection 3.5) compares the dosimetric performance of scintillation detectors to those of other technologies that have been considered suitable for UHDR applications.

3.1. Linearity

In this subsection, we summarize studies that investigated the linearity of scintillation dosimeters with respect to dose and dose rate. While some works with electrons tested doses up to tens of Gy, many assessed linearity as a function of the total delivered dose by increasing the number of pulses, and verified independence from the average dose rate by varying the PRF, without changing either the dose per pulse or the instantaneous dose rate. Here, we focus exclusively on studies in which these two parameters were varied.

3.1.1. Point detectors

The key aspect of the linearity of the scintillator's response as the dose rate increases has been investigated in multiple studies (Tables 1–3). Different types of radiation beams and accelerator machines have been used. Most of the research has been carried out with electron beams in the 6–18 MeV energy range. The UHDR regime was achieved both with conventional LINACs suitably modified, with mobile accelerators (developments of systems originally dedicated to intraoperative radiotherapy, IORT), and with accelerator machines specifically designed and built for preclinical FLASH RT studies. Some studies were also conducted with very high energy electrons (VHEE, up to 200 MeV). The remaining works used protons, typically accelerated in cyclotrons, and X-rays produced by modified X-ray tubes, or in UHDR pulsed X-ray facilities.

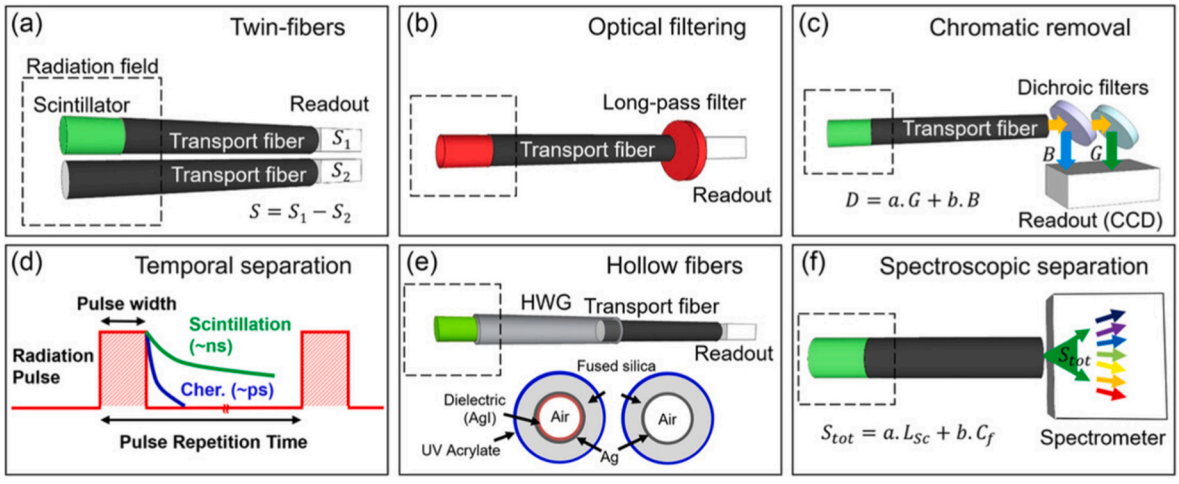

Fig. 3. Methods for Cerenkov contribution mitigation or correction: a) double-fibre method, b) optical filtering, c) chromatic removal, d) temporal separation, e) hollow fibres, f) spectroscopic separation (reproduced from Darafsheh et al. (2024), licensed under CC BY).

Table 1
Summary of the studies evaluating the linearity under UHDR irradiation of organic scintillator point detectors (BCT = beam current transformer, SSD = source to surface distance).

Organic scintillator	Photodetector/ acquisition system	Type of UHDR beam	Investigated range of linearity	Method for dose/ dose rate validation	Remarks	Reference
Proprietary PS-based material (Medscint)	Array of photodetectors of the Hyperscint RP200 scintillation dosimetry system (Medscint)	200 MeV electron beam at CLEAR	DPP: (~5–90) Gy IDR: (~0.22–4.6) · 10^9 Gy/s	Radiochromic film (MD-V3)	Loss of linearity for DPP above ~ 45 Gy, corresponding to IDR ~8 · 10^8 Gy/s	Giguère et al. (2025)
PS-based, BCF-12 (Luxium Solutions)						
PVT-based, EJ-212 (Eljen Technology)						
Hyperscint RP-FLASH (Medscint)	Cooled 2D photodetector array of the RP-FLASH scintillation dosimetry system (MedScint)	18 MeV electron beam (converted LINAC, Varian)	DPP: (0.8–2.3) Gy by varying the SSD	Radiochromic film (EBT-XD)	The scintillator-to-film dose ratio decreased by approximately 4% in a near-linear manner suggesting an under-response of the scintillator with increasing DPP	Guo et al. (2025)
Hyperscint RP-FLASH (Medscint)	Cooled 2D photodetector array of the RP-FLASH scintillation dosimetry system (MedScint)	9 MeV electron beam (Mobetron FLASH electron linear accelerator, IntraOp)	DPP: (0.36–7.7) Gy IDR: (0.086–1.6) · 10^6 Gy/s (at a constant PW of 4 μs by varying the SSD)	Radiochromic film (EBT3) and BCTs of the accelerator dose monitoring system	Reduction in the signal per unit dose of 6% with increasing the DPP/IDR in the investigated range	Baikalov et al. (2025)
PS-based, SCSF-78J (Kuraray)	Back-thinned, back-illuminated CCD camera (Hamamatsu ORCAII-BT-512G)	9 MeV electron beam (ElectronFlash, SIT Sordina IORT Technology)	DPP: (0.3–9.8) Gy IDR: (~0.37–2.4) · 10^6 Gy/s (at a constant PW of 4 μs)	Flash diamond detector (PTW)	Satisfactory linearity in the investigated range	Ciarrocchi et al. (2024)
PS-based, SCSF-3HF (1500) (Kuraray)						
Proprietary PVT-based material	Array of photodetectors of the Hyperscint RP100 scintillation dosimetry system (Medscint)	200 MeV electron beam at CLEAR	DPP: (~5–162) Gy Train duration: (~8–133) ns IDR: (~0.6–1.2) · 10^9 Gy/s	Radiochromic film (EBT3 and MD-V3)	Linear light output with a DPP up to 59.5 Gy. Loss of linearity at higher DPP	Hart et al. (2024)
PS-based, BCF-12 (Luxium Solutions)					Linear light output with a DPP up to 125.2 Gy. Loss of linearity at higher DPP	
Exradin W2 (BCF-12) (Standard Imaging), model dimension 1 mm × 1 mm	Photodetectors of the MAX SD electrometer (Standard Imaging)	9 MeV electron beam (Mobetron FLASH electron linear accelerator, IntraOp)	DPP: (0.5–6.3) Gy (at a constant PW of 3.6 μs by varying the SSD)	Radiochromic film (EBT3) and BCTs of the accelerator dose monitoring system	Loss of linearity of the blue and green signals for DPP> 1.5 Gy	Liu et al. (2024b)
Exradin W2 (BCF-12) (Standard Imaging), model dimension 1 mm × 1 mm and 1 mm × 3 mm	Photodetectors of the MAX SD electrometer (Standard Imaging)	16 MeV electron beam (converted LINAC, FLEX, Varian)	Up to 3.6 Gy/pulse	Radiochromic film (EBT-XD)	Loss of linearity of signal from the 1 mm × 3 mm W2 for DPP> 0.8 Gy (single pulse). The 1 mm × 1 mm W2 scintillator maintained linearity up to the maximum tested DPP	Oh et al. (2024)
Exradin W1 (Standard Imaging)	Photodiode coupled to a real-time embedded industrial controller	10 MeV electron beam (converted LINAC, Varian)	DPP: (0.3–1.1) Gy	Radiochromic film	Satisfactory agreement with the radiochromic film response in the investigated range	Ashraf et al. (2022)
PS-based scintillator	PMT and a Keysight B2985A electrometer	18 MeV protons, cyclotron (IBA)	Average dose rate in the range (30–780) Gy/s	Faraday cup and radiochromic film	Dose rate independence, based on linearity of response to varying beam currents	Casolaro et al. (2022)
PS-based, BCF-10 (Luxium Solutions)	Hyperscint RP100 scintillation dosimetry system (Medscint)	X-rays (80, 100, 120) kVp from a modified x-ray tube (Comet)	Up to 7.1 Gy/s	MC calculation	Dose rate independence, based on linearity of response to varying tube currents	Hart et al. (2022)
PVT-based, EJ-212 (Eljen Technology)	Photodiode (SM05PD7A, Thorlabs) connected to an electrometer (Keithley model 617)	9 MeV electron beam (ElectronFlash, SIT Sordina IORT Technology)	DPP: (0.5–12.5) Gy (at a constant PW of 4 μs by varying the SSD and the applicator diameter)	Radiochromic film	Loss of linearity for DPP above ~ 6 Gy	Morrocchi et al. (2022)
PS-based, BCF-60 (Luxium Solutions)	Spectrometer (Maya, 2000 Pro, Ocean Insight)	6 MeV electron beam (DIRAMS LINAC)	DPP: (0.43–3.16) Gy (at a constant PW of 2.78 μs by varying the SSD)	Radiochromic film (MD-V3)	Satisfactory linearity in the investigated range	Jeong et al. (2021)

Table 2
Summary of the studies evaluating the linearity under UHDR irradiation of inorganic scintillator point detectors (IC = ionization chamber, TLD = thermoluminescent dosimeter, MC = Monte Carlo).

Inorganic scintillator	Photodetector/ acquisition system	Type of UHDR beam	Investigated range of linearity	Method for dose/ dose rate validation	Remarks	Reference
(Y,Yb)AG with different Yb concentrations	Thermoelectric cooled back-thinned CCD array integrated into a spectrometer (PrimeTM X, B&WTec Inc)	9 MeV electron beam (ElectronFlash, SIT Sordina IORT Technology)	DPP: (0.13–9) Gy IDR: (~0.0325–2.25) · 10^6 Gy/s at a constant PW of 4 μs	BCTs of the accelerator dose monitoring system	Satisfactory linearity in the investigated range for the (Y,Yb)AG sample with 50% Yb concentration. Partial loss of linearity above 6 Gy/pulse for the other samples	Cova et al. (2025)
Ce-doped silica-based optical fibres	PMT (Hamamatsu H7421)	74 MeV proton beam, cyclotron (BL2C beam-line of the TRIUMF PTRC)	Up to ~ 36 Gy/s (dose in water)	MC calculation	Dose rate independence, based on linearity of response to varying beam currents	Fricano et al. (2024)
N-doped silica-based optical fibres						
ZnS:Ag	Shamrock 163 spectrometer (Andor Technology) connected to a Lucas S CCD (Andor Technology)	9 MeV electron beam (Mobetron FLASH electron linear accelerator, IntraOp)	DPP: (0.5–6.35) Gy by varying the SSD or PW	BCTs of the accelerator dose monitoring system	Linear response up to 6.35 Gy/ pulse. At DPP of 2.45 Gy (PW = 4 μs and maximum SSD), the signal slightly deviated from the linear trend (probably due to sub-optimal collimation)	Tho and Beddar (2024)
ZnSe:O	Si photomultipliers (MicroFC-SMTPA-60035, SensL)	250 MeV PBS proton beam (ProBeam, Varian)	IDR in the range of 7–1270 Gy/s	IC and calculation from beam current and the spot-to-detector distance	All detectors showed non-linear response with under-response for high IDR	Kanouta et al. (2022)
LYSO	Photodiode SM05PD7A (Thorlabs) connected to a Keithley model 617 electrometer	9 MeV electron beam (ElectronFlash, SIT Sordina IORT Technology)	DPP: (0.5–12.5) Gy, at a constant PW of 4 μs by varying the SSD and the applicator diameter	Radiochromic film	Loss of linearity above ~ 3.5 Gy/ pulse	Morrocchi et al. (2022)
Al2O3:C, Mg	PMT coupled with a data acquisition card (National Instruments)	9 MeV electron beam (ElectronFlash, SIT Sordina IORT Technology)	DPP: (~0.5–4.25) Gy by varying PW and SSD	Radiochromic film and alanine	Loss of linearity above ~ 1 Gy/ pulse	Vanreusel et al. (2022)
Al2O3:C						
Y2O3:Eu (DoseVue standard version and an experimental variant)	Photodetector of the DoseWire 200 system (DoseVue)					
N-doped silica optical fibres	PMT coupled with a photon counting unit	40 keV-19 MeV X-rays originated by and multiple sources (LabHX X-ray machine, ELSA and AXTERIX facilities from CEA)	Dose rates in the range ~ 10^{-2}-10^9 Gy/s in SiO_2	TLDs and Ionization chamber	Linear dose-rate dependence over the investigated range	Vidalot et al. (2022)
Gd_2O_2S:Tb	Hyperscint RP200 scintillation dosimetry system (Medscint)	80 kVp X-rays from a modified x-ray tube (Comet)	Up to ~ 61.27 Gy/s	MC calculation	Dose rate independence, based on linearity of response to varying tube currents	Shaharuddin et al. (2021)
La_2O_2S:Tb						
La_2O_2S:Eu						
Y2O3:Eu	Photodetector of the DoseWire 100 system (DoseVue)	10 MeV electron beam (IORT dedicated electron linear accelerator NOVAC11, in a non-clinical configuration)	DPP up to ~12.5 Gy	Radiochromic film (EBT-XD)	Loss of linearity above ~ 1 Gy/ pulse	Di Martino et al. (2020)

Table 3
Summary of the studies evaluating the linearity under UHDR irradiation of hybrid scintillator point detectors.

Hybrid scintillator	Photodetector/ acquisition system	Type of UHDR beam	Investigated range of linearity	Method for dose/ dose rate validation	Remarks	Reference
$(C_{38}H_{34}P_2)MnCl_4$	PMT coupled with a data acquisition card (National Instruments)	9 MeV electron beam (ElectronFlash, SIT Sordina IORT Technology)	DPP: (~0.5–4.25) Gy by varying PW and SSD	Radiochromic film and alanine	Decreased response with increasing DPP above ~ 2 Gy/pulse	Vanreusel et al. (2022)
$(C_{38}H_{34}P_2)MnBr_4$						
Lead-doped plastic scintillators with different Pb concentrations	Hyperscint RP100 scintillation dosimetry system (Medscint)	X-rays (80, 100, 120) kVp from a modified x-ray tube (Comet)	Up to 40.1 Gy/s	MC calculation	Dose rate independence, based on linearity of response to varying tube currents	Hart et al. (2022)

With UHDR electron beams of a few MeV, the organic scintillators that showed the widest linearity range, up to a DPP of about 10 Gy, corresponding to an IDR on the order of $2.4 \cdot 10^6$ Gy/s, are the plastic scintillating fibres SCSF-78J and SCSF-3HF (Kuraray, Japan) (Ciarrocchi et al., 2024). In the case of irradiations with VHEE beams at 200 MeV, an extended linearity was observed up to at least 45 Gy, corresponding to an IDR on the order of $8 \cdot 10^8$ Gy/s, for proprietary PS-based material (Medscint, Canada), for PS-based BCF-12, and for PVT-based EJ-212 (Giguère et al., 2025). Among inorganic scintillators tested with UHDR electron beams of a few MeV, Yb-admixed yttrium aluminium garnet (YAG) crystals (Cova et al., 2025) and ZnS:Ag powder-based scintillators (Tho and Beddar, 2024) demonstrated the widest linearity range, up to at least 6 Gy of DPP, corresponding to an IDR of approximately $1.5 \cdot 10^6$ Gy/s. Tables 1–3 summarize the main studies about the linearity of point scintillation detectors with respect to dose rate, referring to organic, inorganic, and hybrid scintillators, respectively.

It is important to emphasize that the observed loss of linearity at doses of a few Gy per pulse in most studies quoted in Tables 1–3 is likely due to saturation of the photodetector and electronic readout chain, rather than to the scintillator. This is also evident when comparing results from studies conducted with the same scintillators but coupled to different acquisition systems (e.g., EJ212 tested by Morrocchi et al. (2022, 2025) and by Giguère et al. (2025)). Among the organic scintillators of Table 1, the most investigated are commercial systems already in use in CONV RT, in particular the Exradin W1 and W2 (Standard Imaging, USA) and the Hyperscint platforms (Medscint, Canada). Also the tests with these systems clearly showed that, beyond the scintillator material itself, the signal detection and processing play a fundamental role in extending linearity levels in UHDR regimes, and the limits observed have led to upgrades (Liu et al., 2024b; Oh et al., 2024) and to the implementation of FLASH-dedicated prototypes (Baikalov et al., 2025; Guo et al., 2025).

3.1.2. 2D detectors

To some extent, the linearity of the scintillator signal with the dose per pulse and the dose rate has also been investigated for thin 2D screens. A summary of the studies is reported in Table 4. Most have used inorganic scintillators, but some tests have also been performed with the organic counterpart or with hybrid materials. Since the main advantage of a 2D scintillator is the possibility of imaging the dose profile, these works all used scientific cameras, based on either CMOS or CCD sensors, and some sort of optics for light collection. In several cases, intensifiers have been employed both to amplify the signals and to synchronize and gate the acquisition with the beam pulses. Irradiations have been performed with UHDR electron beams (8–16 MeV) or with high-energy protons (227–250 MeV), mainly produced by cyclotrons. Dose-linearity has been assessed with respect to reference measurements with radiochromic films, ion chambers, point scintillator, Fadaray cup, edge diode, or flash diamond detectors. Organic PVT-based scintillators have been irradiated with both 9-MeV electrons (Morrocchi et al., 2025) and 250 MeV PBS protons (Kanouta et al., 2024), and linearity was observed in both cases. With inorganic scintillators, the highest dose of 50 Gy was reached by Vasyltsiv et al. (2025) with a 250 MeV PBS proton beam, suggesting linearity of the proprietary BaFBr-based detector when compared to radiochromic film readings.

Table 4
Summary of the studies evaluating the linearity under UHDR irradiation of 2D scintillation detectors (iCMOS = intensified CMOS, WET = water equivalent thickness, I = proton beam current).

Type of scintillator	Scintillator name and thickness	Photodetector/ acquisition system	Type of UHDR beam	Investigated range of linearity	Method for dose/ dose rate validation	Remarks	Reference
Organic	PVT-based, EJ212, (Eljen Technology), 0.5 mm	CCD camera (Andor iXon Ultra 888)	9 MeV electron beam (ElectronFlash, SIT Sordina IORT Technology)	DPP: (0.2–12) Gy; IDR: (0.05–3) · 10^6 Gy/s	Flash Diamond (PTW)	Linear response in the tested range	Morrocchi et al. (2025)
Organic	PVT-based, EJ240G, (Eljen Technology), 1 mm	iCMOS camera (DoseOptics)	250 MeV PBS proton beam, isochronous cyclotron	IDR up to 100 Gy/s	Fibre-coupled scintillator	Linearity observed, residuals within 4%	Kanouta et al. (2024)
Inorganic	Proprietary array of Blue-800 BaFBr elements, WET = 1.1 mm[a]	iCMOS camera (DoseOptics)	250 MeV PBS proton beam, cyclotron (Varian ProBeam)	Dose: (2–50) Gy	Radiochromic film (EBT XD)	High linearity with the y-intercept not being forced to zero, but including it in the uncertainty bounds	Vasyltsiv et al. (2025)
Inorganic	Proprietary ImageDosis system with 12% YAG:Ce scintillator coating, 0.1 mm	C-BLUE ONE camera (First Light Imaging)	9 MeV electron beam (ElectronFlash, SIT Sordina IORT Technology)	DPP up to 2 Gy	Radiochromic film (EBT XD or EBT-3)	Response independent from the DPP up to 2 Gy, measured as the ratio of the scintillator to film doses	Vanreusel et al. (2024a)
Inorganic	Rapidex, 0.2 mm (Scintacor)	iCMOS camera (DoseOptics)	250 MeV PBS proton beam, cyclotron (Varian ProBeam)	Dose: (2–22) Gy I: (40–210) nA	Ion chamber (PPC05, IBA)	Linear response in the tested range	Clark et al. (2024)
Inorganic	Blue 800, 0.2 mm (PJ Xray)	iCMOS camera (DoseOptics)	227.7 MeV PBS proton beam, synchrocyclotron (IBA ProteousONE S2C2)	Dose up to 1 Gy I: up to 2 nA	Current monitoring system, intensity calibration to dose with radiochromic film (EBT3)	Image intensity was found linear with respect to current	Clark et al. (2023)
Hybrid	Proprietary hybrid material, WET = 0.7 mm for 8-MeV electrons	CMOS camera (“*CamE*”)	8 MeV electron beam (NDRL)	DPP: (0.28–7.9) Gy, IDR: (0.3–8) · 10^9 Gy/s ADR: (8.4–237) Gy/s	Faraday cup electrode	The highest data point falls 6% below the fit line, slightly exceeding one standard deviation	Levin et al. (2024)

[a] Thin, flexible scintillator proposed for 3D surface dosimetry.

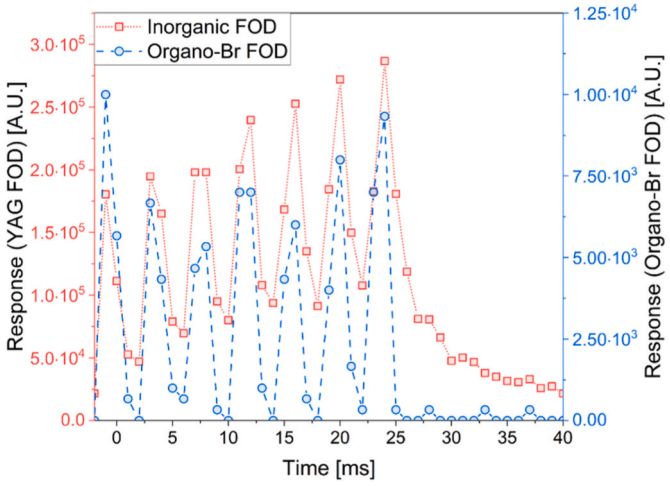

Fig. 4. Time response of two PSD prototypes, an inorganic YAG-based one, and a hybrid one, to irradiations with UHDR electrons, with 245 Hz PRF (reproduced from Vanreusel et al. (2024b), licensed under CC BY).

3.2. Time and spatial performance

3.2.1. Point detectors

Most of the studies to date that report on the temporal performance of scintillators for FLASH RT have been carried out with UHDR electron beams. *In vivo* dose measurements of 10 MeV electron pulses produced by a converted LINAC (Varian Medical Systems, USA) during mice experiments were reported by Ashraf et al. (2022). They used the plastic scintillator from the Exradin W1 system (Standard Imaging, USA), coupled with a gated integrating amplifier and a real-time controller for dose monitoring and feedback control. When the cumulative dose was compared with radiochromic film, the W1 showed an under-response of approximately 3%.

Pulse-by-pulse dose discrimination has also been demonstrated using inorganic and hybrid scintillators. Vanreusel et al. (2024b) showed that both $Y_3Al_5O_{12}:Ce^{3+}$ (YAG) and $(C_{38}H_{34}P_2)MnBr_4$ (Organo-Br) scintillators were able to discriminate 9 MeV electron pulses delivered by an ElectronFlash accelerator (SIT Sordina IORT Technology, Italy) up to the maximum tested PRF of 245 Hz. However, partial pulse overlap was observed with the YAG scintillator due to its longer decay time compared with the Organo-Br scintillator, as shown in Fig. 4. The same study also showed that the Hyperscint RP-200 scintillation dosimetry system (Medscint, Canada) could discriminate pulses only up to a PRF of 4 Hz, due to limitations in the sampling rate associated with spectral binning.

Indeed, beyond the properties of the scintillator itself, the coupled photodetector and associated electronics must be able to acquire and process the signal within sufficiently short timescales. Examples of how the acquisition chain can influence the accurate measurement of single-pulse doses in UHDR electron beams are provided by Poirier et al. (2022) and Baikalov et al. (2025), with respect to the Hyperscint RP-100 system and its successor, the RP-FLASH (Medscint, Canada). In these systems, when the multichannel photodetector readout coincides with pulse delivery, part of the signal is lost. While this phenomenon does not affect the measurement of the total dose of a pulsed beam, it does alter the peak heights of individual pulses, requiring proper correction.

Regarding the possibility of using scintillation dosimeters to monitor the IDR, Ciarrocchi et al. (2024) performed an analysis of the single-pulse structure of 9 MeV electrons at different DPP values, delivered by an ElectronFlash accelerator (SIT Sordina IORT Technology, Italy). They used a SCSF-78J scintillating fibre (Kuraray, Japan) with a decay time of 2.8 ns. A photodiode (DET10A2, Thorlabs, USA) coupled with custom front-end electronics was employed for signal acquisition. The scintillating fibre successfully reproduced the pulse time structure, revealing variations in the IDR consistent with the reference signal provided by the LINAC monitoring system. The slight variation in the dose profile shape and tail were attributed to spurious luminescence with a longer decay time than that of the scintillator.

Several studies on UHDR electron beams have also investigated the possible influence of varying the PRF on the response of scintillation dosimeters. In general, PRF dependencies can be considered negligible, at least for the organic scintillators tested to date. The dependences reported in the literature, and more generally the temporal performance of scintillation dosimeters under UHDR conditions, cannot be attributed solely to the scintillation mechanism itself, but are influenced by multiple factors, including the characteristics of the UHDR beam (dose per pulse, pulse repetition frequency, number of delivered pulses, and pulse duration), the intrinsic properties of the scintillator (e.g., scintillation decay times and afterglow), and the performance of the full detection and acquisition chain, including the method for stem-effect (Cerenkov) removal.

Vanreusel et al. (2022), tested different scintillating materials (Al_2O_3:C; Al_2O_3:C,Mg; Y_2O_3:Eu; $(C_{38}H_{34}P_2)MnCl_4$; and $(C_{38}H_{34}P_2)MnBr_4$) irradiated with 9 MeV electron beams (ElectronFlash, SIT Sordina IORT Technology, Italy), and showed that the response of point scintillators with luminescence decay times longer than the inter-pulse interval (e.g., Al_2O_3:C; Al_2O_3:C,Mg) decreases by more than 50% when increasing the PRF from 1 Hz up to ~250 Hz. Afterward, using the same UHDR beams, Vanreusel et al. (2024b) compared plastic, hybrid, and inorganic scintillators and reported dose measurement variations of approximately 40% for an inorganic scintillator ($Y_3Al_5O_{12}:Ce^{3+}$) and of approximately 10% for a hybrid one ($(C_{38}H_{34}P_2)MnBr_4$, Organo-Br). In contrast, significantly smaller variations within 1% were observed for the PSD Hyperscint RP-200 (Medscint, Canada) when the PRF was varied up to 250 Hz.

Variations below ±1% in the response of the Hyperscint RP-FLASH (Medscint, Canada) were also reported by Baikalov et al. (2025) when varying the average dose rate of a 9 MeV electron beam (Mobetron FLASH electron LINAC, IntraOp, USA) by adjusting the PRF between 5 and 120 Hz. Similar variations, within ±2%, were observed with the same system by Guo et al. (2025) in the PRF range of 30–180 Hz using an 18 MeV electron beam from a converted LINAC (Varian, USA).

The impact of the PRF on the signal response of the PSD W2 (Exradin, Standard Imaging, USA) was analysed by Liu et al. (2024b) for PRF values ranging from 10 to 120 Hz with 9 MeV electron beams (Mobetron FLASH electron LINAC, IntraOp, USA). For a dose per pulse of 1.21 Gy, the variation in the blue channel signal (i.e., dominated by scintillation plus stem effect) remained below 2% across the entire PRF range. At higher doses per pulse, however, a progressive and significant decrease in signal (up to 30%) with increasing PRF was observed. The green channel signal (i.e., mostly stem effect) proved more stable up to 90 Hz independent of the dose per pulse, but dropped by up to 20% at 120 Hz. The authors hypothesized that this signal degradation as a function of dose per pulse and PRF was due to limitations in the electrometer's signal processing rather than the plastic scintillator itself. This PRF dependence of the PSD W2 response was not observed by Oh et al. (2024) when irradiated with 16 MeV electron beams (converted LINAC, FLEX, Varian, USA) at PRFs between 18 and 180 Hz. No significant variations in the response of point inorganic scintillator detectors were also observed by Cova et al. (2025) in Yb-doped YAG scintillators irradiated with 9 MeV electron beams (ElectronFlash, SIT Sordina IORT Technology, Italy) over the PRF range of 1–250 Hz. Similarly, Tho and Beddar (2024), studying a ZnS:Ag scintillator irradiated with 9 MeV electron beams (Mobetron FLASH electron LINAC, IntraOp, USA), observed response variations of less than 0.5% for PRF values up to 120 Hz.

Regarding UHDR beams other than electrons, Kanouta et al. (2022) studied the time structure in PBS proton FLASH treatments using a detector based on ZnSe:O inorganic scintillating crystals. With

sub-millisecond temporal resolution, this system enabled measurements of spot durations and transition times across different scanning directions. A characterization of the commercial PSD system Hyperscint RP-100 (Medscint, Canada) was performed by Poirier et al. (2025) using UHDR PBS proton beams. The authors evaluated the dose and time linearity and demonstrated the capability to experimentally measure the average dose rate and the time-resolved IDR. For pulsed X-rays, Vidalot et al. (2022) demonstrated that radioluminescent nitrogen–silica-doped optical fibers can temporally resolve X-ray pulses separated by intervals of about 1 s, generated at the ELSA (Electrons et Laser, Sources X et Applications) facility.

3.2.2. 2D detectors

Scintillating screens have often been used to monitor the transversal (or longitudinal) dose profile by imaging the scintillation emission with a scientific camera, thus acting as beam monitors or quality control systems. In some cases, commercial devices such as the Lynx-PT (IBA Dosimetry, Germany) have been employed, but several efforts have been dedicated also to developing custom prototypes for FLASH RT applications. Thanks to their radiation hardness, most research has been centred around inorganic scintillators, but commercial organic products have also been studied, in the attempt to exploit their nearly water and tissue-equivalence, or hybrid materials have been developed to try combining the advantages of both types. Often, 2D scintillators have been used for relative dose assessments, but sometimes a conversion of the image pixel values to dose has been provided after a calibration with a reference detector. Depending on the geometry of the light collection, different spatial calibration methods for pixel inhomogeneities (e.g. flat field correction) or geometrical distortions (e.g. oblique view angle) have been needed. Moreover, if combined with ultra-fast cameras, the images have been able to provide both the spatial and the temporal information on the dose delivery. This is particularly useful for proton PBS beams produced by synchrocyclotrons, where the combination of the temporal pulse structure of synchrocyclotrons and the PBS spatial delivery results in a complex spatiotemporal dose distribution, requiring simultaneously high spatial and temporal resolutions. In most cases, radiochromic films have been used as a reference detector to verify the 2D dose profiling capabilities, due to their apparent geometrical similarities with thin scintillator sheets.

Clark et al. (2023) implemented a scintillator-camera system for real-time ultra-high dose rate validation of pulsed synchrocyclotron proton beams. The system spatial performance was verified with several methods, showing an agreement within 1 mm in the x-y beam profile vs single-spot radiochromic film, and of roughly (0.5–0.6) mm in the spot localization compared to the log files, also in a clinical brain patient plan. A similar improved system has later been used by the same group (Clark et al., 2024) to image dose and dose rate maps with PBS UHDR protons, finding an agreement: (i) of (0.2 ± 0.1) mm in the imaged vs planned spot positions, (ii) of (0.2 ± 0.1) ms in the total irradiation time, and (iii) within 3% and 5% in the dose rate with respect to reference measurements and simulations, respectively. In this work, the authors highlight the importance of correctly mapping the dose in the entire field with concurrent high spatiotemporal resolution (sub-millimetric and sub-millisecond, respectively), as the dose rate may vary by up to 5% across regions due to the complicated pattern of PBS beams, potentially leading to areas that fall below the threshold for the FLASH effect. Interestingly, the same imaging system can also be mounted on an endoscope for *in vivo* pulse-by-pulse surface dose monitoring (Clark et al., 2025). Although the apparatus still needs some improvements, e.g., to image the full field with no obstructions, the proposed approach showed encouraging results, because in addition to providing dose and beam structure, this configuration allows to visualize the treatment field before, during, and after the delivery, to verify compliance of the delivery with the plan.

Rahman et al. (2021) irradiated a Gd_2O_2S:Tb screen with a UHDR 10 MeV electron beam to investigate its surface dosimetry capabilities, also in comparison to superficial Cerenkov dosimetry of the irradiated phantom itself. Radiochromic films were used as a reference. Gamma analysis with 3%/3 mm acceptance criteria showed a pass rate of 98.9% for the scintillator, performing significantly better than superficial Cerenkov dosimetry (88.9%). Levin et al. (2024) compared the beam profiling capabilities of a custom hybrid scintillator to those of radiochromic films, using both UHDR proton and electron beams, and showing how the profiles measured with both detectors can be described by the same analytical function with fitting parameters matching within less than 6%.

Vanreusel et al. (2024a) tested the dose profiling capabilities of an in-house imaging system employing a YAG:Ce scintillating material, using low energy UHDR electrons and three circular applicators, with 18, 100, and 120 mm nominal diameters. The penumbra and FWHM of the dose profiles differed from those measured with films, by no more than 3.6% for the FWHM, and significantly for the penumbra. In Morrocchi et al. (2025), an organic scintillator screen was placed parallel to the 9-MeV UHDR electron beam axis, and the luminescence was imaged from a side, through a transparent plastic layer mimicking a water phantom surrounding the scintillator. Although preliminary, this study showed one of the main potential advantages of scintillator screens, that is the possibility to obtain in a single image, on a per-pulse basis, and almost in real time the full bidimensional dose distribution. From the acquired image, a profile along the beam axis can be selected to derive the percentage-depth-dose curve. Here, even without correcting for the Cerenkov contribution in the collected light, the extracted depth-dose curve gave dosimetric beam parameters compatible within a few percents with those measured with radiochromic films.

As for VHEE, Rieker et al. (2024) compared a custom, YAG scintillator-based beam profile monitoring system to radiochromic films, and proposed a procedure for dose calibration of the scintillator reading. The tested system provided transversal beam profiles that differed by roughly 5%–10% from those measured with films, but the authors foresee a better agreement after optimizing the camera parameters.

The capability of using scintillating screens for time-resolved 2D beam monitoring has been demonstrated also during *in vivo* experiments on mice legs immersed in a water tank, by placing the transparent scintillating sheet behind the irradiated leg to image the proton PBS spot positions and field profile, indicating an agreement with radiochromic films within 0.4 mm (Kanouta et al., 2024). An example acquisition is reported in Fig. 5, showing the measured instantaneous (Fig. 5a) and cumulative (Fig. 5b) dose maps acquired with the scintillator at three time points during proton PBS irradiations. The black dashed line shows the progress of the dose delivery. Fig. 5c and d show the instantaneous and cumulative intensity for the two positions indicated in Fig. 5a and b by the red and black stars, respectively. Prior to that, Kourkafas et al. (2021) had already visualized the transverse proton beam profile with a radioluminescent screen and CCD camera before *in vivo* mouse eye experiments, but in that case the scintillator was used as pre-irradiation quality assurance system, and not as a real-time tool during the experiments. Recently, also Vanreusel et al. (2025) has tested two flexible inorganic scintillators and two cameras, using a converted LINAC to produce 16 MeV UHDR electrons in a preclinical setting, for future *in vivo* dosimetry studies, showing robust (i.e., within 5%) readings among the various tested combinations of scintillators and cameras.

Finally, Darafsheh and Bey (2025) supported the implementation of a proton FLASH synchrocyclotron platform for preclinical experiments by measuring the beam lateral 2D profiles with a stand-alone Lynx PT system (IBA Dosimetry, Germany), i.e., with no reference detector, observing no geometrical distortions or dependence on dose rate, for four different UHDR values.

3.2.3. 3D detectors

Very few studies so far have investigated the feasibility of reconstructing the 3D dose distribution using scintillators. In Ravera et al. (2024a), a method using a scintillator monolith imaged along four

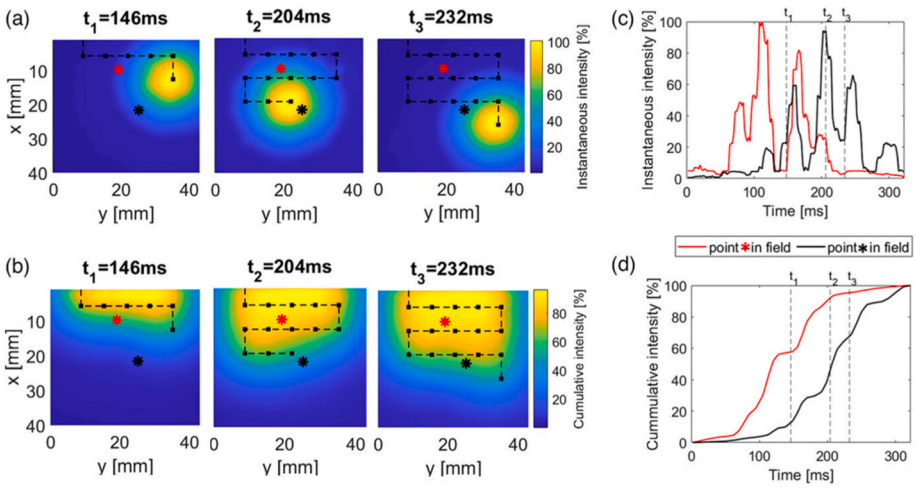

Fig. 5. Representative set of images of the dose distribution of a proton PBS irradiation acquired, with a scintillator sheet. a) Instantaneous dose images at three time points. b) Cumulative dose images. The dotted line with square points shows the beam position at each timestamp. Instantaneous (c) and cumulative (d) image intensities as a function of time, for the two positions indicated by the red and black stars in (a) and (b) (reproduced from Kanouta et al. (2024), licensed under CC BY). (For interpretation of the references to colour in this figure legend, the reader is referred to the Web version of this article.)

projections and a maximum likelihood expectation maximization was tested on a dose distribution simulated with Geant4, suggesting deviations smaller than 20% from the expected dose, with the largest differences closer to high dose gradients. Also, a preliminary, proof-of-concept image of a 10-cm side EJ200 plastic scintillating block was acquired with an optical imaging system, under 9-MeV UHDR electron irradiation. Pizzardi et al. (2025) have imaged a single projection of a scintillator block (in this case, with 5 cm side), and used the cylindrical symmetry of the dose distribution and an iterative inverse Abel transform algorithm to reconstruct the dose distribution. The results were compared to radiochromic films and TOPAS Monte Carlo simulations, suggesting good qualitative agreement.

A completely different approach was suggested by Vasyltsiv et al. (2025), who developed and characterized a thin and flexible array of hexagonal inorganic BaFBr scintillators for potential use in clinical 3D surface dosimetry. A stereovision imaging system composed of three cameras allowed to transform the dose distribution to the reference frame of the treatment planning system and to correct for the angular dependencies introduced by the imaging system. The suggested approach was able to retrieve the dose distribution with an average localization error of 0.62 mm, better than the accepted clinical tolerance of 1 mm, and an uncertainty on the dose measurement of roughly 1%.

3.3. Radiation damage

3.3.1. Point detectors

The body of literature on the medium-to long-term effects of UHDR beams on the luminescent and dosimetric properties of scintillation dosimeters is becoming increasingly substantial. However, to the authors' knowledge, it remains largely limited to organic scintillators, especially commercial systems such as the W1, W2 (Standard Imaging, USA), and Hyperscint platforms (Medscint, Canada). Findings across studies are not always in full agreement. These discrepancies should be interpreted in the context of methodological differences in irradiation conditions, including beam quality, dose rate, total irradiation time, accumulated dose, recovery intervals, and the pre-irradiation history of the dosimeters. All of these factors can affect the medium-to long-term response of the detector systems. Furthermore, in point scintillation dosimeters using an optical fibre as light guide, radiation-induced damage affects not only the scintillator itself but also the optical fibre, complicating the interpretation and comparison of results.

In general, it can be stated that although exposure to high doses and high dose rates inevitably produces damage to plastic scintillators

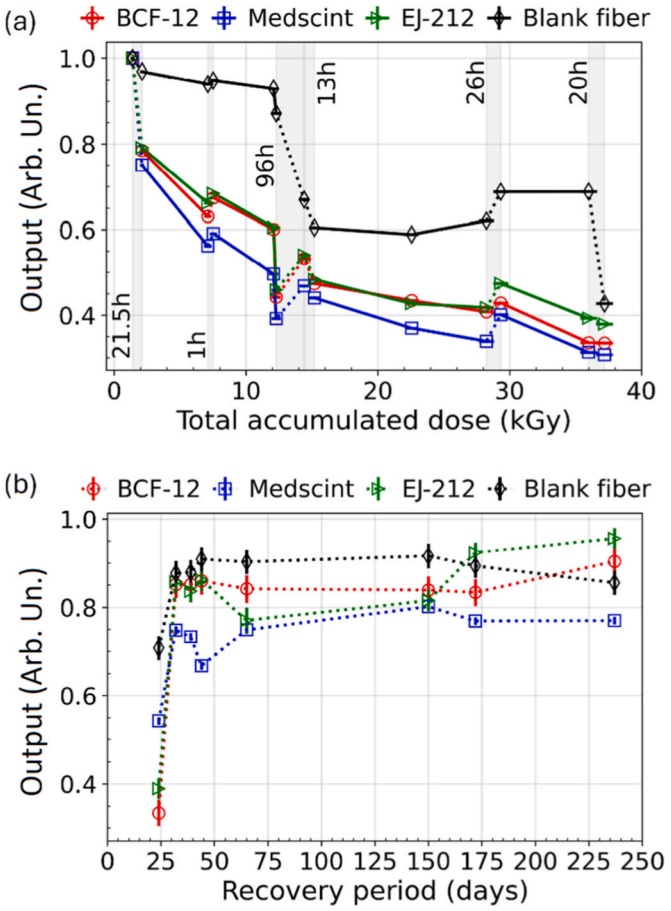

Fig. 6. Radiation damage as a function of the total accumulated dose (a) and output recovery as a function of the recovery period (b), for three commercial plastic scintillators (BCF-12, Medscint, and EJ212) and for an optical fibre (adapted from Giguère et al. (2025), licensed under CC BY).

and/or light guides, this damage is often at least partially reversible over time. From a strictly dosimetric perspective, the loss of sensitivity following irradiation could be faced by tracking the accumulated dose of each dosimeter and performing periodic recalibrations to correct for

progressive sensitivity loss.

The radiation hardness of scintillators coupled to Hyperscint RP100, RP200, and RP-FLASH systems has been evaluated by Hart et al. (2024), Giguère et al. (2025) and Guo et al. (2025), respectively. The first two studies employed 200 MeV UHDR electron beams, whereas the latter used 18 MeV electrons. Hart et al. (2024) observed that after delivering a dose of 13.8 kGy, the light output of the proprietary PVT-based Medscint material was reduced by approximately 20% (~1.5%/kGy). This efficiency loss was comparable to that observed in a PS-based BCF-12 scintillator irradiated up to 26.2 kGy under similar experimental conditions.

Similar results were reported by Giguère et al. (2025), who used the same UHDR beam of Hart et al. (2024) and investigated not only radiation-induced damage but also signal recovery over time. The investigated samples included proprietary PS-based Medscint material, PVT-based EJ-212 scintillator, PS-based BCF-12 scintillating optical fibre, and PMMA optical fibre. The results of Giguère et al. (2025) demonstrated that, after 37.2 kGy, the final light output decreased to approximately 30–43% of the initial response, as reported in Fig. 6a. The measured light yield losses were approximately 1.8%/kGy, 1.9%/kGy, 1.7%/kGy, and 1.5%/kGy for BCF-12, Medscint, EJ-212, and blank fibre, respectively. Notably, for the scintillators, the rate of light output loss was higher for the first kGys of accumulated dose, with a decrease of more than 20% between 1.4 kGy and 2.1 kGy, while it was much lower and approximately constant after about 10 kGy. Radiation damage also induced a spectral shift toward longer (yellowish) wavelengths. During the experiments, Giguère et al. (2025) introduced rest intervals between successive irradiations, allowing the evaluation of short-term recovery. At 7.1 kGy and 1 h rest, recovery rates were ~4.6%/h for BCF-12, 2.7%/h for Medscint, 1.9%/h for EJ-212, and 0.64%/h for blank fibre. At 28.2 kGy and 26 h rest, recovery rates decreased to 0.076, 0.23, 0.25, and 0.26%/h, respectively. This indicates that recovery depends both on rest duration and on accumulated dose. Long-term recovery was significant, stabilizing after 32 days (BCF-12), 150 days (Medscint), 172 days (EJ-212), and 32 days (blank fibre), as shown in Fig. 6b. After stabilization, residual permanent damage to light output (6–22%) remained, although spectral recovery was complete.

In the study by Guo et al. (2025), a total dose of ~10 kGy was delivered to the scintillator of the Hyperscint RP-FLASH system within 2 h. After irradiation, the light output was reduced to ~80% of the initial value. The signal loss was not linear over the entire dose range and was modeled with a second-order polynomial. Between 0 and 2 kGy, the loss rate was ~2.6%/kGy, whereas it was smaller at higher doses.

For the commercial Exradin W1 dosimeter (Standard Imaging, USA), Ashraf et al. (2022) assessed radiation damage using 10 MeV UHDR electron beams. They tracked sensitivity over time and periodically recalibrated the Cerenkov correction factor and gain values to quantify changes. A sensitivity loss of ~16%/kGy was observed up to ~1 kGy, followed by a lower decay rate of ~7% up to 3 kGy. Partial recovery was observed between experiments conducted 5 days apart. The degradation rate reported by Ashraf et al. (2022) was significantly higher than values reported under CONV RT dose rates for the same dosimeter. For example, Carrasco et al. (2015) derived W1 long-term stability from calibration coefficient changes up to 127 kGy, observing a sensitivity loss of ~0.28%/kGy for 0–15 kGy, and ~0.032%/Gy beyond 15 kGy. Dimitriadis et al. (2017) reported an initial ~8% drop (1.6%/kGy) in the first 5 kGy, followed by ~0.2%/kGy over the next 20 kGy. The datasheet of the Exradin W2 dosimeter (evolution of W1), provided by the vendor (Standard Imaging, USA) currently reports a radiation degradation of ~2%/kGy.

Radiation damage rates from Ashraf et al. (2022) were also much higher than those observed by Liu et al. (2024b) for the W2 dosimeter under 9 MeV UHDR electron beams. In this study, signal sensitivity was tracked up to 8.5 kGy, with hourly measurements taken over 8 h. The results showed sensitivity losses of ~4%/kGy in the blue channel and 0.3%/kGy in the green channel, more in line with results from plastic scintillators irradiated in conventional beamlines.

A systematic study of W2 radiation damage under 9 MeV UHDR electron beams was conducted by Tho et al. (2025), reaching 12 kGy total accumulated dose. Experiments involved nine W2 dosimeters. The scintillator and the portion of the optical fibre coupled to the scintillator exposed to the UHDR radiation field were selectively shielded with lead thicknesses to distinguish between the radiation damage contribution due to the optical guide and that of the scintillator. In addition, three blank PMMA optical guide fibres (i.e. without the scintillator element) were tested. When only the scintillator was exposed to UHDR beams, average sensitivity losses were ~2%/kGy (blue channel) and ~0.5%/kGy (green channel). When only the optical fibre was irradiated, i.e., by shielding the scintillating element, losses increased to ~6%/kGy (blue channel) and ~1%/kGy (green channel). For bare PMMA fibres, the blue-channel luminescence decreased by ~1%/kGy, with negligible loss in the green channel. Two months after irradiation, recovery measurements showed mean recovery of 10–18% for the blue channel in W2, but an additional 16–18% loss in the green channel. PMMA fibres also exhibited mainly blue-channel recovery of ~12–14%. Overall, the results of Tho et al. (2025) suggested that, compared to existing literature, scintillators exposed to UHDR beams exhibited higher sensitivity loss than under conventional dose rate beams. Moreover, the contribution of the optical guide to total sensitivity loss cannot be neglected. The authors' recommendation was that users should monitor cumulative dose and recalibrate after every ~2 kGy to ensure accurate readings.

3.3.2. 2D detectors

To the best of our knowledge, so far only one study has investigated the radiation hardness of scintillators in the form of 2D screens, and no results are yet available for 3D blocks, for which the research is still immature. In Levin et al. (2024), the radiation hardness of a proprietary hybrid scintillator screen has been assessed with a quasi-continuous scanning proton pencil beam. The measurement was done by setting a high DPP = (8.0 ± 0.4) Gy/pulse, PRF = 30 Hz and acquiring data continuously for 15 min, giving a total time-averaged dose rate (240 ± 12) Gy/s and a total cumulative dose of 216 kGy. The used metrics was the ratio of the pixel charge in ADC counts in the beam centre relative to the counts in a very low dose control region (1% of the primary region). A 0.025%/kGy signal decrease was observed.

3.4. Spurious luminescence

Spurious luminescence is an intrinsic phenomenon that affects scintillators and optically transparent materials in general, regardless of the dose rate with which they are irradiated. Many studies in the field of FLASH scintillation dosimetry have investigated the relevance of this contribution and how effective the compensation methods can be. In the following, we summarize the several approaches adopted and the main conclusions that have been reached. As for the other aspects, most of the research has been dedicated to point detectors, but a few studies on other geometries are also starting to appear.

3.4.1. Point detectors

With point detectors, the main contribution to spurious light is the Cerenkov luminescence produced in the optical fibre, which can be mitigated or corrected using one of the methods described in the previous Section 2.4.4. Many studies have been performed with commercial devices, that already implement one of these (Ashraf et al., 2022; Guo et al., 2025; Liu et al., 2024b; Oh et al., 2024; Poirier et al., 2022; Shaharuddin et al., 2021). In some cases, e.g. with proton beams, the Cerenkov contribution could be neglected, and only fluorescence of the optical fibre determined the stem effect (Poirier et al., 2025; Fricano et al., 2024; Kanouta et al., 2022).

Also studies testing non-commercial devices for FLASH RT dosimetry have adopted similar methods. For example, in Vanreusel et al. (2024b), the reduction of the stem signal of the in-house prototypes was studied

with three optical bandpass filters, centred around 425, 500, and 525 nm, and either 50 or 80 nm wide. The 500-nm filter, with the largest width, returned the pulse length value closest to the expectation and was thus considered the most suitable for the tested prototypes. Moreover, the stem signal contribution was measured by varying the portion of optical fibre that was irradiated, but the results were inconclusive and the authors suggest further investigation with a spectrometer.

Another possible simple approach is shifting the fibre detector so that the scintillating tip is far away from the beam, and only a portion of the optical fibre is irradiated. This allows estimating the Cerenkov light ratio after correcting for the actual irradiated fibre length (Ciarrocchi et al., 2024; Hart et al., 2024). Moreover, Ravera et al. (2024b) proposed a method to inter-calibrate five scintillating-fibre detectors, accounting also for their position-dependent Cerenkov contribution.

In Cova et al. (2025), the stem effect in (Y,Yb)AG-based fibre detectors was studied as a function of the relative orientation of the beam with respect to the fibre axis, showing a strong dependence on the orientation angle, but also on the portion of irradiated optical fibre. This work has also highlighted the advantage of choosing scintillators with emission at long wavelengths (above 900 nm in their case) to minimize the Cerenkov contribution.

3.4.2. 2D detectors

Vanreusel et al. (2024a) discussed how the Cerenkov radiation produced in the phantom, especially when transparent, can add up to the signal of their inorganic scintillator and cause a dose overestimation, and how this contribution can be mitigated in fibre detectors or 2D applications, using spectral analysis and optical filters, respectively.

Morrocchi et al. (2025) proposed a method to isolate the scintillation light from the Cerenkov contribution by using a set of two optical narrow bandpass filters, a blue one to collect mostly scintillation photons, and a green one to maximize Cerenkov light. They then formulated a linear system of two equations, much like in the chromatic removal approach for fibres, describing the signals in the blue and green wavelength bands as a linear combination of the two contributions, which can be solved to yield the scintillation contribution alone. This method, applied to images acquired by placing the plastic scintillator after layers of water-equivalent plastic of increasing thickness, provided a percentage depth dose curve for 9-MeV UHDR electrons that was visibly much closer to that of a reference flash diamond detector, especially in the first 15 mm, the dose build-up region.

3.5. Comparison with other dosimeters

The comparison of scintillation detectors with other available technologies has been partially discussed in previous papers. Ashraf et al. (2020) highlighted the capability of luminescent detectors to perform 1D, 2D, and 3D dosimetry with sub-millimetric spatial resolution, nanosecond temporal resolution, and dose-rate independence up to 10^5 Gy/s. Romano et al. (2022) outlined the characteristics of various dosimeters, indicating scintillators as capable of real-time and *in vivo* dosimetry, potentially suitable for reference dosimetry and beam monitoring, and available in 2D configurations such as fibre arrays or sheets. The same work also pointed out quenching in high-LET fields and Cerenkov radiation as potential issues.

More recently, Oh et al. (2024) summarized the advantages and limitations of both traditional (radiochromic films, optically-stimulated luminescence detectors, thermoluminescent detectors, alanine, and ion chambers) and innovative (ultra-thin ion chambers, diamond detectors, calorimeters and beam-current transformers) detectors for UHDR applications. However, a detailed comparison of scintillators with other technologies was beyond the scope of that work. Here, we provide an updated synthesis based on the full body of literature currently available.

Scintillators offer several key advantages: as active devices, they enable real-time dose measurements without post-processing, unlike passive detectors such as radiochromic films. When coupled with suitable photodetectors and readout electronics, they exhibit a linear response with dose and dose rate, often outperforming standard ionization chambers. In addition, organic scintillators are nearly water-equivalent, requiring few corrections for dose-to-water conversion, and they are sufficiently fast to resolve the pulse structure and IDR of UHDR beams.

Conversely, their response is strongly dependent on the irradiation geometry and conditions. This makes them suitable for relative dose measurements, but the determination of a dose value in Gy is less straightforward than for calorimeters, modified ionization chambers, or diamond detectors. Radiation hardness, particularly for organic materials, may also be inferior to that of other detector types. Despite these limitations, scintillating screens have demonstrated a unique capability for real-time, single-pulse, single-shot two-dimensional dosimetry of UHDR beams, a functionality that remains unmatched by other technologies and may prove crucial for the future development of FLASH radiotherapy, including from a radiation protection perspective.

4. Conclusions and future perspectives

This review has highlighted that, over the past five years, research on the development and characterization of scintillators for FLASH dosimetry and monitoring has been particularly active. Most studies have focused on fibre-coupled point detectors and on systems for two-dimensional characterization of radiation fields, whereas investigations addressing three-dimensional dose measurements remain limited, reflecting the greater complexity of 3D dosimetry.

For point-based systems, research has focused on commercial PSDs and their recent evolutions, especially regarding the acquisition electronics for UHDR conditions. In parallel, several groups have explored inorganic materials of various compositions, while hybrid point scintillators have been investigated less extensively. A similar distribution among materials is observed in 2D dosimetry, with a predominance of inorganic materials, fewer studies on organic screens, and a minority on hybrid solutions. Unlike point detectors, the reduced availability of commercial 2D devices, currently limited to a single inorganic option, to the best of our knowledge, has encouraged the use of commercial materials in combination with custom readout systems, as well as the development of proprietary solutions. For 3D dosimetry, the few experimental results involved a commercial plastic scintillator and an inorganic-based proprietary detector.

Overall, most studies have shown that scintillation dosimeters can be useful for dosimetry and monitoring of UHDR beams. They are therefore instruments that, alongside other technologies of different nature and operating principles, can contribute to the standardization of FLASH irradiation parameters, thereby helping to clarify the mechanisms of the FLASH effect and supporting clinical translation.

Some aspects still require further investigation, with radiation hardness being among the most critical. Despite the available literature, results are sometimes partially conflicting, reflecting the dependence of radiation damage on multiple parameters, including scintillator history, cumulative dose, dose rate, radiation quality, exposure and recovery times. More standardized studies should be carried out under conditions closely replicating those expected in FLASH RT. At present, most radiation hardness data have been gathered only as secondary outcomes of other investigations, performed under highly variable irradiation conditions and recovery times. This limitation applies not only to plastic scintillators but also to inorganic and hybrid ones, for which data on radiation hardness under UHDR beams relevant to FLASH RT remain especially scarce.

Regarding the management of the Cerenkov emission and the stem effect in fibre-based devices, the existing literature indicates that the strategies established in CONV RT, such as chromatic removal and hyperspectral analysis, may also be applied under UHDR conditions, provided that appropriate precautions are taken with respect to

radiation-induced damage. Medium-to long-term radiation effects, and the corresponding repair dynamics, can in fact affect different spectral regions of the light signal reaching the photodetector, requiring careful periodic validation and adjustment of correction and calibration factors. Moreover, the direct extension of approaches for point detectors to 2D and 3D configurations still has to be proven, as these geometries introduce different geometrical dependences that may require further corrections. Finally, alternative Cerenkov mitigation strategies, including time filtering and the use of air-core fibres, merit further investigation, as they have shown promise in previous CONV-RT studies, despite not being yet implemented in commercial dosimetry systems.

With respect to scintillator response as a function of dose and dose rate, available evidence confirms that the composition and scintillation mechanisms of the material influence the linearity range, but the photodetector and the signal-processing electronics play an equally important role. This interdependence complicates direct comparisons among scintillators tested in the literature, since even for the same material, the achievable temporal resolution and dynamic range are determined by the entire detection chain. Moreover, the detection system must balance all requirements necessary for accurate dosimetric signal collection, meaning that high temporal resolution may compromise other needs. For instance, wavelength-resolved acquisition methods used to discriminate the signal of interest from the stem effect typically require longer acquisition times.

From a materials standpoint, commercially available plastic scintillators, including scintillating fibres, already represent viable tools for high-temporal-resolution dose measurements, owing to their fast scintillation times and radiological water-equivalence, provided that Cerenkov discrimination is effective and medium-to long-term radiation damage is carefully considered. Inorganic scintillators, by contrast, offer a broader range of compositions and scintillation properties, including long-wavelength emitters in the red or infrared regions, which may help mitigating radiation damage associated with colour centres that mainly absorb in the UV spectral region, and facilitate the reduction of the spurious luminescence through spectral methods.

Future research on point-based detectors should also prioritize the development and testing of hybrid scintillators under UHDR irradiation conditions, with a particular focus on temporal performance and radiation hardness to enable direct comparison with the more extensively studied plastic scintillators. For 2D dosimetry, research seems to be moving towards systems with simultaneous spatial and temporal capabilities, a feature particularly valuable for capturing the complex spatio-temporal dose distributions typical of proton PBS therapy. In this context, efforts are directed not only toward the selection of the fastest scintillating materials, but also toward the optimization of the readout chain, including the camera triggering, gating, and, most critically, the frame rate, which often represents the main limiting factor in the temporal performance of an optical imaging system.

Finally, there is a rising interest in detectors capable of performing dosimetry *in vivo* during FLASH RT. Some of the studies published to date have already started showing that this is feasible both with point and 2D scintillators. Still, conclusions on their capabilities and limitations for these applications are far from being drawn.

CRediT authorship contribution statement

Esther Ciarrocchi: Writing – review & editing, Writing – original draft, Methodology, Investigation, Conceptualization. **Ivan Veronese:** Writing – review & editing, Writing – original draft, Methodology, Investigation, Conceptualization.

Declaration of competing interest

I. Veronese is a Senior Associate Editor for this journal and was not involved in the editorial review or the decision to publish this article.

Data availability

Data will be made available on request.

References

Anand, A., Zaffalon, M.L., Erroi, A., Cova, F., Carulli, F., Brovelli, S., 2024. Advances in perovskite nanocrystals and nanocomposites for scintillation applications. ACS Energy Lett. 9 (3), 1261–1287. https://doi.org/10.1021/acsenergylett.3c02763. American Chemical Society.

Archambault, L., Therriault-Proulx, F., Beddar, S., Beaulieu, L., 2012. A mathematical formalism for hyperspectral, multipoint plastic scintillation detectors. Phys. Med. Biol. 57 (21), 7133–7145. https://doi.org/10.1088/0031-9155/57/21/7133.

Archer, J., Li, E., Davis, J., Cameron, M., Rosenfeld, A., Lerch, M., 2019. High spatial resolution scintillator dosimetry of synchrotron microbeams. Sci. Rep. 9 (1). https://doi.org/10.1038/s41598-019-43349-6.

Ashraf, M.R., Rahman, M., Cao, X., Duval, K., Williams, B.B., Jack Hoopes, P., Gladstone, D.J., Pogue, B.W., Zhang, R., Bruza, P., 2022. Individual pulse monitoring and dose control system for pre-clinical implementation of FLASH-RT. Phys. Med. Biol. 67 (9). https://doi.org/10.1088/1361-6560/ac5f6f.

Ashraf, M.R., Rahman, M., Zhang, R., Williams, B.B., Gladstone, D.J., Pogue, B.W., Bruza, P., 2020. Dosimetry for FLASH radiotherapy: a review of tools and the role of radioluminescence and cherenkov emission. In: Frontiers in Physics, 8. Frontiers Media SA. https://doi.org/10.3389/fphy.2020.00328.

Ayotte, G., Archambault, L., Gingras, L., Lacroix, F., Beddar, A.S., Beaulieu, L., 2006. Surface preparation and coupling in plastic scintillator dosimetry. Med. Phys. 33 (9), 3519–3525. https://doi.org/10.1118/1.2256300.

Baikalov, A., Tho, D., Liu, K., Bartzsch, S., Beddar, S., Schüler, E., 2025. Characterization of a time-resolved, real-time scintillation dosimetry system for ultra-high dose-rate radiation therapy applications. Int. J. Radiat. Oncol. Biol. Phys. 121 (5), 1372–1383. https://doi.org/10.1016/j.ijrobp.2024.11.092.

Beaulieu, L., Beddar, S., 2016. Review of plastic and liquid scintillation dosimetry for photon, electron, and proton therapy. Phys. Med. Biol. 61 (20), R305. https://doi.org/10.1088/0031-9155/61/20/R305.

Beddar, A.S., Mackie, T.R., Attix, F.H., 1992a. Cerenkov light generated in optical fibres and other light pipes irradiated by electron beams. Phys. Med. Biol. 37 (4), 925–935. https://doi.org/10.1088/0031-9155/37/4/007.

Beddar, A.S., Mackie, T.R., Attix, F.H., 1992b. Water-equivalent plastic scintillation detectors for high-energy beam dosimetry: II. Properties and measurements. Phys. Med. Biol. 31 (1O), 1901–1913. https://doi.org/10.1088/0031-9155/37/10/007.

Beddar, A.S., Mackie, T.R., Attix, F.H., 1992c. Water-equivalent plastic scintillation detectors for high-energy beam dosimetry: I. Physical characteristics and theoretical considerations. Phys. Med. Biol. 37 (10), 1883–1900. https://doi.org/10.1088/0031-9155/37/10/006.

Beddar, S., Beaulieu, L. (Eds.), 2016. Scintillation Dosimetry, first ed. CRC Press. https://doi.org/10.1201/9781315372655.

Birks, J.B., 1951. Scintillations from organic crystals: specific fluorescence and relative response to different radiations. Proc. Phys. Soc. 64 (10), 874. https://doi.org/10.1088/0370-1298/64/10/303.

Butler, D.J., Barnes, M., McEwen, M.R., Lerch, M.L.F., Sheehy, S.L., Tan, Y.R.E., Williams, I.M., Yap, J.S.L., 2025. Dosimetry for FLASH and other non-standard radiotherapy sources. Radiat. Meas. 180. https://doi.org/10.1016/j.radmeas.2024.107330.

Carrasco, P., Jornet, N., Jordi, O., Lizondo, M., Latorre-Musoll, A., Eudaldo, T., Ruiz, A., Ribas, M., 2015. Characterization of the Exradin W1 scintillator for use in radiotherapy. Med. Phys. 42 (1), 297–304. https://doi.org/10.1118/1.4903757.

Casolaro, P., Dellepiane, G., Gottstein, A., Mateu, I., Scampoli, P., Braccini, S., 2022. TIME-RESOLVED proton beam dosimetry for ultra-high dose-rate cancer therapy (flash). Proceedings of the International Beam Instrumentation Conference, IBIC, pp. 519–521. https://doi.org/10.18429/JACoW-IBIC2022-WE3C2.

Ciarrocchi, E., Belcari, N., 2017. Cerenkov luminescence imaging: physics principles and potential applications in biomedical sciences. EJNMMI Phys. 4 (1). https://doi.org/10.1186/s40658-017-0181-8. Springer International Publishing.

Ciarrocchi, E., Ravera, E., Cavalieri, A., Celentano, M., Del Sarto, D., Di Martino, F., Linsalata, S., Massa, M., Masturzo, L., Moggi, A., Morrocchi, M., Pensavalle, J.H., Bisogni, M.G., 2024. Plastic scintillator-based dosimeters for ultra-high dose rate (UHDR) electron radiotherapy. Phys. Med. 121. https://doi.org/10.1016/j.ejmp.2024.103360.

Clark, M., Daniel, N., Bruza, P., Zhang, R., Jarvis, L., Hoopes, P.J., Gladstone, D., 2025. Imaging system for real-time, full-field pulse-by-pulse surface dosimetry of UHDR electron beams. Med. Phys. 52 (6), 5026–5031. https://doi.org/10.1002/mp.17784.

Clark, M., Ding, X., Zhao, L., Pogue, B., Gladstone, D., Rahman, M., Zhang, R., Bruza, P., 2023. Ultra-fast, high spatial resolution single-pulse scintillation imaging of

synchrocyclotron pencil beam scanning proton delivery. Phys. Med. Biol. 68 (4). https://doi.org/10.1088/1361-6560/acb753.
Clark, M., Harms, J., Vasyltsiv, R., Sloop, A., Kozelka, J., Simon, B., Zhang, R., Gladstone, D., Bruza, P., 2024. Quantitative, real-time scintillation imaging for experimental comparison of different dose and dose rate estimations in UHDR proton pencil beams. Med. Phys. 51 (9), 6402–6411. https://doi.org/10.1002/mp.17247.
Clift, M.A., Johnston, P.N., Webb, D.V., 2002. A temporal method of avoiding the Cerenkov radiation generated in organic scintillator dosimeters by pulsed mega-voltage electron and photon beams. Phys. Med. Biol. 47 (8), 1421. https://doi.org/10.1088/0031-9155/47/8/313.
Cova, F., Morrocchi, M., Fasoli, M., Ciarrocchi, E., Pensavalle, J.H., Gallo, S., Cavalieri, A., Zhang, M., Zhang, K., Jia, Z., Tonelli, M., Di Martino, F., Vedda, A., Bisogni, M.G., Veronese, I., 2025. Stem effect-free (Y,Yb)AG-based detectors for ultra-high dose rate electron beam dosimetry. Sensor Actuator Phys. 390. https://doi.org/10.1016/j.sna.2025.116539.
Darafsheh, A., Bey, A., 2025. Implementation of a proton FLASH platform for pre-clinical studies using a gantry-mounted synchrocyclotron. Phys. Med. Biol. 70 (10). https://doi.org/10.1088/1361-6560/add106.
Darafsheh, A., Goddu, S.M., Williamson, J., Zhang, T., Sobotka, L.G., 2024. Radioluminescence dosimetry in modern radiation therapy. Adv. Photon. Res. 5 (9). https://doi.org/10.1002/adpr.202300350.
de Boer, S.F., Beddar, A.S., Rawlinson, J.A., 1993. Optical filtering and spectral measurements of radiation-induced light in plastic scintillation dosimetry. Phys. Med. Biol. 38 (7), 945. https://doi.org/10.1088/0031-9155/38/7/005.
Di Martino, F., Barca, P., Barone, S., Bortoli, E., Borgheresi, R., De Stefano, S., Di Francesco, M., Grasso, L., Lucia, G., Linsalata, S., Marfisi, D., Pacitti, M., Migliorati, M., Felici, G., Palumbo, L., Faillace, L., 2020. FLASH radiotherapy with electrons: issues related to the production, monitoring, and dosimetric characterization of the beam. Front. Phys. 8. https://doi.org/10.3389/fphy.2020.570697.
Di Martino, F., Del Sarto, D., Bass, G., Capaccioli, S., Celentano, M., Coves, D., Douralis, A., Marinelli, M., Marrale, M., Masturzo, L., Milluzzo, G., Montefiori, M., Paiar, F., Pensavalle, J.H., Raffaele, L., Romano, F., Subiel, A., Touzain, E., Verona Rinati, G., Felici, G., 2023. Architecture, flexibility and performance of a special electron linac dedicated to flash radiotherapy research: electronflash with a triode gun of the centro pisano flash radiotherapy (CPFR). Front. Phys. 11. https://doi.org/10.3389/fphy.2023.1268310.
Di Martino, F., Del Sarto, D., Giuseppina Bisogni, M., Capaccioli, S., Galante, F., Gasperini, A., Linsalata, S., Mariani, G., Pacitti, M., Paiar, F., Ursino, S., Vanreusel, V., Verellen, D., Felici, G., 2022. A new solution for UHDP and UHDR (Flash) measurements: theory and conceptual design of ALLS chamber. Phys. Med. 102, 9–18. https://doi.org/10.1016/j.ejmp.2022.08.010.
Di Martino, F., Giannelli, M., Traino, A.C., Lazzeri, M., 2005. Ion recombination correction for very high dose-per-pulse high-energy electron beams. Med. Phys. 32 (7), 2204–2210. https://doi.org/10.1118/1.1940167.
Diffenderfer, E.S., Sørensen, B.S., Mazal, A., Carlson, D.J., 2022. The current status of preclinical proton FLASH radiation and future directions. Med. Phys. 49 (3), 2039–2054. https://doi.org/10.1002/mp.15276.
Dimitriadis, A., Patallo, I.S., Billas, I., Duane, S., Nisbet, A., Clark, C.H., 2017. Characterisation of a plastic scintillation detector to be used in a multicentre stereotactic radiosurgery dosimetry audit. Radiat. Phys. Chem. 140, 373–378. https://doi.org/10.1016/j.radphyschem.2017.02.023.
Dujardin, C., Auffray, E., Bourret-Courchesne, E., Dorenbos, P., Lecoq, P., Nikl, M., Vasil'Ev, A.N., Yoshikawa, A., Zhu, R.Y., 2018. Needs, trends, and advances in inorganic scintillators. IEEE Trans. Nucl. Sci. 65 (8), 1977–1997. https://doi.org/10.1109/TNS.2018.2840160.
Dujardin, C., Bessière, A., Bulin, A.L., Chaput, F., Mahler, B., 2025. Inorganic nanoscintillators: current trends and future perspectives. Adv. Opt. Mater. 13 (12). https://doi.org/10.1002/adom.202402739. John Wiley and Sons Inc.
Esplen, N., Mendonca, M.S., Bazalova-Carter, M., 2020. Physics and biology of ultrahigh dose-rate (FLASH) radiotherapy: a topical review. Phys. Med. Biol. 65 (23). https://doi.org/10.1088/1361-6560/abaa28. IOP Publishing Ltd.
Farr, J., Grilj, V., Malka, V., Sudharsan, S., Schippers, M., 2022. Ultra-high dose rate radiation production and delivery systems intended for FLASH. Med. Phys. 49 (7), 4875–4911. https://doi.org/10.1002/mp.15659.
Favaudon, V., Caplier, L., Monceau, V., Pouzoulet, F., Sayarath, M., Fouillade, C., Poupon, M.-F., Brito, I., Hupé, P., Bourhis, J., Hall, J., Fontaine, J.-J., Vozenin, M.-C., 2014. Ultrahigh dose-rate FLASH irradiation increases the differential response between normal and tumor tissue in mice. Sci. Transl. Med. 6 (245), 245ra93. https://doi.org/10.1126/scitranslmed.3008973, 245ra93.
Folkerts, M.M., Abel, E., Busold, S., Perez, J.R., Krishnamurthi, V., Ling, C.C., 2020. A framework for defining FLASH dose rate for pencil beam scanning. Med. Phys. 47 (12), 6396–6404. https://doi.org/10.1002/mp.14456.
Fontbonne, J.M., Iltis, G., Ban, G., Battala, A., Vernhes, J.C., Tillier, J., Bellaize, N., Le Brun, C., Tamain, B., Mercier, K., Motin, J.C., 2002. Scintillating fiber dosimeter for radiation therapy accelerator. IEEE Trans. Nucl. Sci. 49 I (5), 2223–2227. https://doi.org/10.1109/TNS.2002.803680.
Fricano, F., Morana, A., Lambert, D., Hoehr, C., Campanella, C., Belanger-Champagne, C., Trinczek, M., El Hamzaoui, H., Capoen, B., Cassez, A., Bouazaoui, M., Melin, G., Robin, T., Boukenter, A., Marin, E., Ouerdane, Y., Paillet, P., Girard, S., 2024. Very high dose rate proton dosimetry with radioluminescent silica-based optical fibers. IEEE Trans. Nucl. Sci. 71 (8), 1829–1836. https://doi.org/10.1109/TNS.2024.3378803.
Gao, Y., Liu, R., Chang, C.W., Charyyev, S., Zhou, J., Bradley, J.D., Liu, T., Yang, X., 2022. A potential revolution in cancer treatment: a topical review of FLASH radiotherapy. J. Appl. Clin. Med. Phys. 23 (10). https://doi.org/10.1002/acm2.13790. John Wiley and Sons Ltd.
Giguère, C., Hart, A., Bateman, J., Korysko, P., Farabolini, W., LeChasseur, Y., Bazalova-Carter, M., Beaulieu, L., 2025. Radiation damage and recovery of plastic scintillators under ultra-high dose rate 200 MeV electrons at CERN CLEAR facility. Phys. Med. Biol. 70 (7). https://doi.org/10.1088/1361-6560/adc234.
Gómez, F., Gonzalez-Castaño, D.M., Fernández, N.G., Pardo-Montero, J., Schüller, A., Gasparini, A., Vanreusel, V., Verellen, D., Felici, G., Kranzer, R., Paz-Martín, J., 2022. Development of an ultra-thin parallel plate ionization chamber for dosimetry in FLASH radiotherapy. Med. Phys. 49 (7), 4705–4714. https://doi.org/10.1002/mp.15668.
Guo, L., Zhou, B., Tsai, Y.C., Jiang, K., Iakovenko, V., Wang, K.K.H., 2025. Comprehensive characterization and validation of a fast-resolving (1000 Hz) plastic scintillator for ultra-high dose rate electron dosimetry. Med. Phys. 52 (10). https://doi.org/10.1002/mp.70006.
Plastic scintillators. In: Hamel, M. (Ed.), 2021. Chemistry and Applications. Springer. https://doi.org/10.1007/978-3-030-73488-6.
Hart, A., Cecchi, D., Giguère, C., Larose, F., Therriault-Proulx, F., Esplen, N., Beaulieu, L., Bazalova-Carter, M., 2022. Lead-doped scintillator dosimeters for detection of ultrahigh dose-rate x-rays. Phys. Med. Biol. 67 (10). https://doi.org/10.1088/1361-6560/ac69a5.
Hart, A., Giguère, C., Bateman, J., Korysko, P., Farabolini, W., Rieker, V., Esplen, N., Corsini, R., Dosanjh, M., Beaulieu, L., Bazalova-Carter, M., 2024. Plastic scintillator dosimetry of ultrahigh dose-rate 200 MeV electrons at CLEAR. IEEE Sens. J. 24 (9), 14229–14237. https://doi.org/10.1109/JSEN.2024.3353190.
Jelley, J.V., 1961. Čerenkov radiation: its origin, properties and applications. Contemp. Phys. 3 (1), 45–57. https://doi.org/10.1080/00107516108204445.
Jeong, D.H., Lee, M., Lim, H., Kang, S.K., Lee, K., Lee, S.J., Kim, H., Han, W.K., Kang, T. W., Jang, K.W., 2021. Optical filter-embedded fiber-optic radiation sensor for ultra-high dose rate electron beam dosimetry. Sensors 21 (17). https://doi.org/10.3390/s21175840.
Kanouta, E., Bruza, P., Johansen, J.G., Kristensen, L., Sørensen, B.S., Poulsen, P.R., 2024. Two-dimensional time-resolved scintillating sheet monitoring of proton pencil beam scanning FLASH mouse irradiations. Med. Phys. 51 (7), 5119–5129. https://doi.org/10.1002/mp.17049.
Kanouta, E., Johansen, J.G., Kertzscher, G., Sitarz, M.K., Sørensen, B.S., Poulsen, P.R., 2022. Time structure of pencil beam scanning proton FLASH beams measured with scintillator detectors and compared with log files. Med. Phys. 49 (3), 1932–1943. https://doi.org/10.1002/mp.15486.
Kapłon, Kulig, D., Beddar, S., Fiutowski, T., Górska, W., Hajduga, J., Jurgielewicz, P., Kabat, D., Kalecińska, K., Kopeć, M., Koperny, S., Mindur, B., Moroń, J., Moskal, G., Niedźwiecki, S., Silarski, M., Sobczuk, F., Szumlak, T., Ruciński, A., 2022. Investigation of the light output of 3D-printed plastic scintillators for dosimetry applications. Radiat. Meas. 158. https://doi.org/10.1016/j.radmeas.2022.106864.
Kharzheev, Y.N., 2019. Radiation hardness of scintillation detectors based on organic plastic scintillators and optical fibers. Phys. Part. Nucl. 50 (1), 42–76. https://doi.org/10.1134/S1063779619010027.
Knoll, G.F., 2010. Radiation Detection and Measurement, fourth ed. Wiley, ISBN 978-0-470-13148-0.
Kourkafas, G., Bundesmann, J., Fanselow, T., Denker, A., Ehrhardt, V.H., Gollrad, J., Budach, V., Weber, A., Kociok, N., Joussen, A.M., Heufelder, J., 2021. FLASH proton irradiation setup with a modulator wheel for a single mouse eye. Med. Phys. 48 (4), 1839–1845. https://doi.org/10.1002/mp.14730.
Lambert, J., Yin, Y., McKenzie, D.R., Law, S., Suchowerska, N., 2008. Cerenkov-free scintillation dosimetry in external beam radiotherapy with an air core light guide. Phys. Med. Biol. 53 (11), 3071–3080. https://doi.org/10.1088/0031-9155/53/11/021.
Large, M.J., Kanxheri, K., Posar, J., Aziz, S., Bashiri, A., Calcagnile, L., Calvo, D., Caputo, D., Caricato, A.P., Catalano, R., Cirio, R., Cirrone, G.A.P., Croci, T., Cuttone, G., De Cesare, G., De Remigis, P., Dunand, S., Fabi, M., Frontini, L., et al., 2024. Dosimetry of microbeam radiotherapy by flexible hydrogenated amorphous silicon detectors. Phys. Med. Biol. 69 (15). https://doi.org/10.1088/1361-6560/ad64b5.
Lecoq, P., Gektin, A., Korzhik, M., 2017. Inorganic Scintillators for Detector Systems. Physical Principles and Crystal Engineering. Springer. https://doi.org/10.1007/978-3-319-45522-8.
Levin, D.S., Friedman, P.S., Ferretti, C., Ristow, N., Tecchio, M., Litzenberg, D.W., Bashkirov, V., Schulte, R., 2024. A prototype scintillator real-time beam monitor for ultra-high dose rate radiotherapy. Med. Phys. 51 (4), 2905–2923. https://doi.org/10.1002/mp.17018.
Li, J., Chen, Q., Zhou, J., Cao, Z., Li, T., Liu, F., Yang, Z., Chang, S., Zhou, K., Ming, Y., Yan, T., Zheng, W., 2024. Radiation damage mechanisms and research status of radiation-resistant optical fibers: a review. Sensors 24 (10). https://doi.org/10.3390/s24103235. Multidisciplinary Digital Publishing Institute (MDPI).
Liu, K., Waldrop, T., Aguilar, E., Mims, N., Neill, D., Delahoussaye, A., Li, Z., Swanson, D., Lin, S.H., Koong, A.C., Taniguchi, C.M., Loo, B.W., Mitra, D., Schüler, E., 2024a. Redefining FLASH radiation therapy: the impact of mean dose rate and dose per pulse in the gastrointestinal tract. Int. J. Radiat. Oncol. Biol. Phys. https://doi.org/10.1016/j.ijrobp.2024.10.009.
Liu, K., Holmes, S., Schüler, E., Beddar, S., 2024b. A comprehensive investigation of the performance of a commercial scintillator system for applications in electron FLASH radiotherapy. Med. Phys. 51 (6), 4504–4512. https://doi.org/10.1002/mp.17030.
Ma, Y., Zhang, W., Zhao, Z., Lv, J., Chen, J., Yan, X., Lin, X.J., Zhang, J., Wang, B., Gao, S., Xiao, J., Yang, G., 2024. Current views on mechanisms of the FLASH effect in cancer radiotherapy. Natl. Sci. Rev. 11 (10). https://doi.org/10.1093/nsr/nwae350. Oxford University Press.

Marinelli, M., di Martino, F., Del Sarto, D., Pensavalle, J.H., Felici, G., Giunti, L., De Liso, V., Kranzer, R., Verona, C., Verona Rinati, G., 2023. A diamond detector based dosimetric system for instantaneous dose rate measurements in FLASH electron beams. Phys. Med. Biol. 68 (17). https://doi.org/10.1088/1361-6560/aead0.

Marinelli, M., Felici, G., Galante, F., Gasparini, A., Giuliano, L., Heinrich, S., Pacitti, M., Prestopino, G., Vanreusel, V., Verellen, D., Verona, C., Verona Rinati, G., 2022. Design, realization, and characterization of a novel diamond detector prototype for FLASH radiotherapy dosimetry. Med. Phys. 49 (3), 1902–1910. https://doi.org/10.1002/mp.15473.

Medina, E., Ferro, A., Abujami, M., Camperi, A., Centis Vignali, M., Data, E., Del Sarto, D., Deut, U., Di Martino, F., Fadavi Mazinani, M., Ferrero, M., Ferrero, V., Giordanengo, S., Martì Villarreal, O.A., Hosseini, M.A., Mas Milian, F., Masturzo, L., Montalvan Olivares, D.M., Montefiori, M., et al., 2024. First experimental validation of silicon-based sensors for monitoring ultra-high dose rate electron beams. Front. Phys. 12. https://doi.org/10.3389/fphy.2024.1258832.

Milluzzo, G., De Napoli, M., Di Martino, F., Amato, A., Del Sarto, D., D'Oca, M.C., Marrale, M., Masturzo, L., Medina, E., Okpuwe, C., Pensavalle, J.H., Vignati, A., Camarda, M., Romano, F., 2024. Comprehensive dosimetric characterization of novel silicon carbide detectors with UHDR electron beams for FLASH radiotherapy. Med. Phys. 51 (9), 6390–6401. https://doi.org/10.1002/mp.17172.

Morrocchi, M., Ciarrocchi, E., Anzalone, R., Cavalieri, A., Martino, F. Di, D'Orazio, C., Massa, M., Moggi, A., Mozzo, C., Pensavalle, J.H., Ravera, E., Bisogni, M.G., 2025. Plastic scintillator sheets for quality assurance in electron FLASH and minibeam radiation therapy. Med. Phys. 52 (8). https://doi.org/10.1002/mp.18033.

Morrocchi, M., Pensavalle, J.H., Ciarrocchi, E., Di Martino, F., Felici, G., Galante, F., Gasparini, A., Grasso, L., Linsalata, S., Massa, M., Moggi, A., Pacitti, M., Vanreusel, V., Verellen, D., Bisogni, M.G., 2022. Experimental characterization and Monte Carlo simulation of scintillator detectors in online electron FLASH radiotherapy dosimetry. J. Instrum. 17 (9). https://doi.org/10.1088/1748-0221/17/09/P09005.

Nikl, M., 2006. Scintillation detectors for x-rays. Meas. Sci. Technol. 17 (4). https://doi.org/10.1088/0957-0233/17/4/R01.

Oancea, C., Sykorova, K., Jakubek, J., Pivec, J., Riemer, F., Worm, S., Bourgouin, A., 2025. Dosimetric and temporal beam characterization of individual pulses in FLASH radiotherapy using Timepix3 pixelated detector placed out-of-field. Phys. Med. 129. https://doi.org/10.1016/j.ejmp.2024.104872.

Oh, K., Hyun, M.A., Gallagher, K.J., Yan, Y., Zhou, S., 2024. Characterization of a commercial plastic scintillator for electron FLASH dosimetry. J. Appl. Clin. Med. Phys. 25 (8). https://doi.org/10.1002/acm2.14451.

Pizzardi, S., Alborghetti, L., Vurro, F., Lacavalla, M.A., Capialbi, M.M., Martino, F. Di, Masturzo, L., Cavalieri, A., Fiorino, C., Spinelli, A.E., 2025. Abstract 4485 radioluminescence 3D dose reconstruction for FLASH radiotherapy using the abel transform. Radiother. Oncol. 206, S2680–S2682. https://doi.org/10.1016/S0167-8140(25)03410-3.

Poirier, Y., Xu, J., Mossahebi, S., Therriault-Proulx, F., Sawant, A., 2022. Technical note: characterization and practical applications of a novel plastic scintillator for online dosimetry for an ultrahigh dose rate (FLASH). Med. Phys. 49 (7), 4682–4692. https://doi.org/10.1002/mp.15671.

Poirier, Y., Byrne, K.E., Hamad, G., Therriault-Proulx, F., Jiang, K., Deng, W., et al., 2025. What's in a proton FLASH beam? Characterizing ultra-high dose rate protons using a commercial plastic scintillator. Radiat. Res. 203 (4), 201–213. https://doi.org/10.1667/RADE-24-00117.1.

Rahman, M., Ashraf, M.R., Zhang, R., Gladstone, D.J., Cao, X., Williams, B.B., Jack Hoopes, P., Pogue, B.W., Bruza, P., 2021. Spatial and temporal dosimetry of individual electron FLASH beam pulses using radioluminescence imaging. Phys. Med. Biol. 66 (13). https://doi.org/10.1088/1361-6560/ac0390.

Ravera, E., Anzalone, R., Cavalieri, A., Ciarrocchi, E., Del Sarto, D., Di Martino, F., Morrocchi, M., Bisogni, M.G., 2024a. A 3D imaging system for dosimetry in FLASH radiotherapy. Nucl. Instrum. Methods Phys. Res. Sect. A Accel. Spectrom. Detect. Assoc. Equip. 1069. https://doi.org/10.1016/j.nima.2024.169910.

Ravera, E., Cavalieri, A., Ciarrocchi, E., Del Sarto, D., Di Martino, F., Massa, M., Masturzo, L., Moggi, A., Morrocchi, M., Pensavalle, J.H., Bisogni, M.G., 2024b. A new calibration method of an array of plastic scintillating fibers for dosimetry in electron FLASH radiotherapy. Radiat. Meas. 177. https://doi.org/10.1016/j.radmeas.2024.107254.

Rieker, V.F., Corsini, R., Stapnes, S., Adli, E., Farabolini, W., Grilj, V., Sjobak, K.N., Wroe, L.M., Aksoy, A., Robertson, C.S., Bateman, J.J., Korysko, P., Malyzhenkov, A., Gilardi, A., Dosanjh, M., 2024. Active dosimetry for VHEE FLASH radiotherapy using beam profile monitors and charge measurements. Nucl. Instrum. Methods Phys. Res. Sect. A Accel. Spectrom. Detect. Assoc. Equip. 1069. https://doi.org/10.1016/j.nima.2024.169845.

Romano, F., Bailat, C., Jorge, P.G., Lerch, M.L.F., Darafsheh, A., 2022. Ultra-high dose rate dosimetry: challenges and opportunities for FLASH radiation therapy. Med. Phys. 49 (7), 4912–4932. https://doi.org/10.1002/mp.15649.

Romano, F., Milluzzo, G., Di Martino, F., D'Oca, M.C., Felici, G., Galante, F., Gasparini, A., Mariani, G., Marrale, M., Medina, E., Pacitti, M., Sangregorio, E., Vanreusel, V., Verellen, D., Vignati, A., Camarda, M., 2023. First characterization of novel silicon carbide detectors with ultra-high dose rate electron beams for FLASH radiotherapy. Appl. Sci. 13 (5). https://doi.org/10.3390/app13052986.

Rosini, G., Ciarrocchi, E., D'Orsi, B., 2025. Mechanisms of the FLASH effect: current insights and advances. In: Frontiers in Cell and Developmental Biology, 13. Frontiers Media SA. https://doi.org/10.3389/fcell.2025.1575678.

Shaharuddin, S., Hart, A., Cecchi, D.D., Bazalova-Carter, M., Foley, M., 2021. Real-time dosimetry of ultrahigh dose-rate x-ray beams using scintillation detectors. Proceedings of IEEE Sensors, 2021-October. https://doi.org/10.1109/SENSORS47087.2021.9639825.

Shevelev, V.S., Ishchenko, A.V., Vanetsev, A.S., Nagirnyi, V., Omelkov, S.I., 2022. Ultrafast hybrid nanocomposite scintillators: a review. In: Journal of Luminescence, 242. Elsevier B.V. https://doi.org/10.1016/j.jlumin.2021.118534.

Tao, L., Feng, S., Yang, Y., Zheng, B., 2025. Dosimetry characteristics of ultra-high dose rate X-ray: a short review. In: Frontiers in Physics, 13. Frontiers Media SA. https://doi.org/10.3389/fphy.2025.1576227.

Tashiro, M., Yoshida, Y., Oike, T., Nakao, M., Yusa, K., Hirota, Y., Ohno, T., 2022. First human cell experiments with FLASH carbon ions. Anticancer Res. 42 (5), 2469–2477. https://doi.org/10.21873/anticanres.15725.

Therriault-Proulx, F., Archambault, L., Beaulieu, L., Beddar, S., 2012. Development of a novel multi-point plastic scintillation detector with a single optical transmission line for radiation dose measurement. Phys. Med. Biol. 57 (21), 7147–7159. https://doi.org/10.1088/0031-9155/57/21/7147.

Tho, D., Beddar, S., 2024. Characterization of an inorganic powder-based scintillation detector under a UHDR electron beam. Sensors 24 (24). https://doi.org/10.3390/s24248064.

Tho, D., Liu, K., Holmes, S., Schüler, E., Beddar, S., 2025. Radiation damage of the W2 plastic scintillator under ultra-high dose rate FLASH electron beam. Radiat. Meas. 187. https://doi.org/10.1016/j.radmeas.2025.107492.

Tinganelli, W., Sokol, O., Quartieri, M., Puspitasari, A., Dokic, I., Abdollahi, A., Durante, M., Haberer, T., Debus, J., Boscolo, D., Voss, B., Brons, S., Schuy, C., Horst, F., Weber, U., 2022a. Ultra-high dose rate (FLASH) carbon ion irradiation: dosimetry and first cell experiments. Int. J. Radiat. Oncol. Biol. Phys. 112 (4), 1012–1022. https://doi.org/10.1016/j.ijrobp.2021.11.020.

Tinganelli, W., Weber, U., Puspitasari, A., Simoniello, P., Abdollahi, A., Oppermann, J., Schuy, C., Horst, F., Helm, A., Fournier, C., Durante, M., 2022b. FLASH with carbon ions: tumor control, normal tissue sparing, and distal metastasis in a mouse osteosarcoma model. Radiother. Oncol. 175, 185–190. https://doi.org/10.1016/j.radonc.2022.05.003.

Vanreusel, V., Brown, S., Ali, S., De Kerf, T., Doemer, A.J., Leblans, P., Movsas, B., Nusrat, H., Shirmard, B., Thind, K., Vanlanduit, S., Verellen, D., Gasparini, A., Nascimento, L. de F., 2025. Characterization and ex vivo application of flexible 2D scintillating coatings in ultra-high dose rate electron beams for FLASH radiotherapy. Preprint. http://arxiv.org/abs/2504.15824.

Vanreusel, V., Gasparini, A., Galante, F., Mariani, G., Pacitti, M., Cociorb, M., Giammanco, A., Reniers, B., Reulens, N., Shonde, T.B., Vallet, H., Vandenbroucke, D., Peeters, M., Leblans, P., Ma, B., Felici, G., Verellen, D., de Freitas Nascimento, L., 2022. Point scintillator dosimetry in ultra-high dose rate electron "FLASH" radiation therapy: a first characterization. Phys. Med. 103, 127–137. https://doi.org/10.1016/j.ejmp.2022.10.005.

Vanreusel, V., Heinrich, S., De Kerf, T., Leblans, P., Vandenbroucke, D., Vanlanduit, S., Verellen, D., Gasparini, A., de Freitas Nascimento, L., 2024a. A dose rate independent 2D Ce-doped YAG scintillating dosimetry system for time resolved beam monitoring in ultra-high dose rate electron "FLASH" radiation therapy. Sensor Actuator Phys. 371. https://doi.org/10.1016/j.sna.2024.115313.

Vanreusel, V., Vallet, H., Wijnen, J., Côté, B., Leblans, P., Sterckx, P., Vandenbroucke, D., Verellen, D., de Freitas Nascimento, L., 2024b. In-Vivo dosimetry for ultra-high dose rate (UHDR) electron beam FLASH radiotherapy using an organic (Plastic), an organic–inorganic hybrid and an inorganic point scintillator system. Photonics 11 (9). https://doi.org/10.3390/photonics11090865.

Vasyltsiv, R., Harms, J., Clark, M., Gladstone, D.J., Pogue, B.W., Zhang, R., Bruza, P., 2025. Design and characterization of a novel scintillator array for UHDR PBS proton therapy surface dosimetry. Med. Phys. 52 (7). https://doi.org/10.1002/mp.17922.

Veronese, I., Andersen, C.E., Li, E., Madden, L., Santos, A.M.C., 2024. Radioluminescence-based fibre-optic dosimeters in radiotherapy: a review. Radiat. Meas. 174. https://doi.org/10.1016/j.radmeas.2024.107125.

Vidalot, J., Campanella, C., Dachicourt, J., Marcandella, C., Duhamel, O., Morana, A., Poujols, D., Assaillit, G., Gaillardin, M., Boukenter, A., Ouerdane, Y., Girard, S., Paillet, P., 2022. Monitoring of ultra-high dose rate pulsed X-ray facilities with radioluminescent nitrogen-doped optical fiber. Sensors 22 (9). https://doi.org/10.3390/s22093192.

Vozenin, M.C., Loo, B.W., Tantawi, S., Maxim, P.G., Spitz, D.R., Bailat, C., Limoli, C.L., 2024. FLASH: new intersection of physics, chemistry, biology, and cancer medicine. Rev. Mod. Phys. 96 (3). https://doi.org/10.1103/RevModPhys.96.035002.

Weber, U.A., Scifoni, E., Durante, M., 2022. FLASH radiotherapy with carbon ion beams. Med. Phys. 49 (3), 1974–1992. https://doi.org/10.1002/mp.15135. John Wiley and Sons Ltd.

Wibowo, A., Sheikh, M.A.K., Diguna, L.J., Ananda, M.B., Marsudi, M.A., Arramel, A., Zeng, S., Wong, L.J., Birowosuto, M.D., 2023. Development and challenges in perovskite scintillators for high-resolution imaging and timing applications. Commun. Mater. 4 (1). https://doi.org/10.1038/s43246-023-00348-5. Springer Nature.

Zhu, D., Nikl, M., Chewpraditkul, W., Li, J., 2022. Development and prospects of garnet ceramic scintillators: a review. J. Adv. Ceram. 11 (12), 1825–1848. https://doi.org/10.1007/s40145-022-0660-9. Tsinghua University.